

UNCLASSIFIED

AD NUMBER
AD805413
NEW LIMITATION CHANGE
TO Approved for public release, distribution unlimited
FROM Distribution authorized to U.S. Gov't. agencies and their contractors; Administrative/Operational Use; 15 JAN 1967. Other requests shall be referred to Aero Propulsion Lab., Wright-Patterson AFB, OH 45433.
AUTHORITY
AFAPL ltr, 12 Apr 1972

THIS PAGE IS UNCLASSIFIED

AD 805413

CONTRACT NO. AF 33(615)-3487

SILVER-ZINC ELECTRODES AND SEPARATOR RESEARCH

Second Quarterly Technical Progress Report

Covering the Period

1 October 1966 to 1 January 1967

Dated

15 January 1967

Prepared by

J. J. Lander

J. A. Keralla

NOTICE

Foreign announcement and distribution of this report is not authorized. Release to the Clearinghouse for Federal Scientific and Technical Information, CFSTI (formerly OTS) is not authorized. The distribution of this report is limited because it contains technology identifiable with items on the Strategic Embargo Lists excluded from export or re-export under U.S. Export Control Act of 1949 (63STAT.7), as amended (50 USC APP 2020.2031), as implemented by AFR. 400-10.

FOREWORD

This report was prepared by Delco-Remy Division of General Motors Corporation, Anderson, Indiana, on Air Force Contract No. AF 33(615)-3487, Silver-Zinc Electrodes and Separator Research. The work was administered under the direction of the Static Energy Conversion Section, Flight Vehicle Power Branch, Aero-Space Power Division, Aero Propulsion Laboratory; Mr. J. E. Cooper was task engineer for the laboratory.

The assistance of Dr. T. P. Dirkse, Professor of Chemistry, Calvin College, Grand Rapids, Michigan, as consultant on this project is greatly appreciated.

This report is being published and distributed prior to Air Force review. The publication of this report, therefore, does not constitute approval by the Air Force of the findings or conclusions contained herein. It is published for the exchange and stimulation of ideas.

TABLE OF CONTENTS

I.	<u>Introduction</u>	Page 1
II.	<u>Factual Data</u>	2
	C. Mechanical Barriers to Zinc Agglomeration .	2
	D. Particle Size and Morphology of Zinc Oxides	3
	E. Zinc Electrode Fabrication Techniques . . .	3
	F. Influence of Membrane Separator Character- istics	4
	I. Sizes of Zincate Ion and Soluble Silver Species in KOH	5
	N. Surfactant Tests	12
III.	<u>Summary</u>	13
	<u>Distribution List</u>	14
	<u>Figures</u>	16
	<u>Appendix</u>	42

LIST OF FIGURES

	Page
Figure 1. Initial Capacity of Cells Containing Various Fibers in Negative Plates	16
Figure 2. Number of Cycles Obtained by Cells in Group 1	17
Figure 3. Number of Cycles Obtained by Cells in Group 2	18
Figure 4. Number of Cycles Obtained by Cells in Group 3	19
Figure 5. Negative Plate Containing 5% FSC Fibers at 146 Cycles	20
Figure 6. Negative Plate Containing 10% FSC Fibers at 146 Cycles	21
Figure 7. Negative Plate Containing 15% FSC Fibers at 146 Cycles	22
Figure 8. Negative Plate Containing 5% Asbestos Fibers at 134 Cycles	23
Figure 9. Negative Plate Containing 10% Asbestos Fibers at 134 Cycles	24
Figure 10. Negative Plate Containing 15% Asbestos Fibers at 134 Cycles	25
Figure 11. Negative Plate Containing 5% Zinc Fibers at 171 Cycles	26
Figure 12. Negative Plate Containing 10% Zinc Fibers at 108 Cycles	27
Figure 13. Negative Plate Containing 15% Zinc Fibers at 168 Cycles	28
Figure 14. Negative Plate of Control Cell for XX-601 and XX-4 Acicular Oxides at 77 Cycles	29
Figure 15. Negative Plate Containing 5% XX-601 ZnO at 77 Cycles	30
Figure 16. Negative Plate Containing 10% XX-601 ZnO at 77 Cycles	31
Figure 17. Negative Plate Containing 2% XX-601 ZnO at 77 Cycles	32
Figure 18. Negative Plate Containing 5% XX-4 ZnO at 157 Cycles	33
Figure 19. Negative Plate Containing 10% XX-4 ZnO at 157 Cycles	34
Figure 20. Number of Cycles Obtained by Cells Using $ZnCO_3$ and $ZnSO_4$ in the Negative Plate	35
Figure 21. Number of Cycles Obtained by Various Surfactants	36
Figure 22. Volume vs. Molality KOH Solutions at 68°F.	37
Figure 23. Non-Ideality of KOH Solutions	38
Figure 24. Vapor Pressure of Solutions of KOH, 68°F.	39
Figure 25. Hydration of KOH, 68°F.	40
Figure 26. Bound Water vs. KOH Concentration. 68°F.	41

ABSTRACT

The use of $ZnSO_4$ in the negative plate mix appears to aid cycle life at 60% depth-of-discharge.

Surfactants tested to date other than Emulphogene BC-610 do not improve cycle life performance at room temperature at 60% depth-of-discharge.

Development of failure analysis techniques are progressing through the use of one media, the photomicrograph.

A first approach to the estimation of degree of molecular hydration in KOH solutions of battery strength is made, and on this basis, limiting values of hydrated ion sizes are calculated.

I. Introduction

The specific items under study in this contract are:

- A. Separators
- B. Electrolytes
- C. Mechanical Barriers to Zinc Agglomeration
- D. Particle Size and Morphology of Zinc Oxides
- E. Zinc Electrode Fabrication Techniques
- F. Influence of Membrane Separator Characteristics
- G. Sites for Zinc Oxide Overgrowth
- H. Development of Failure Analysis Techniques
- I. Sizes of Zincate Ion and Soluble Silver Species in KOH
- J. Membrane Pore Size Measurements in KOH
- K. Stoichiometric Ratio of Formed Zinc
- L. Fundamental Studies on Surfactants
- M. Alternate Method of Surface Area Measurement
- N. Surfactant Tests

This report covers the second three month period on this program.

II. Factual Data

C. Mechanical Barriers to Zinc Agglomeration

Eighty-one 25 a.h. cells were constructed with varying percentages of FSC fibers, asbestos fibers, and zinc fibers in the negative plate mix as follows:

- Group 1 . 9 cells with 5% FSC fibers in negative mix
9 cells with 10% FSC fibers in negative mix
9 cells with 15% FSC fibers in negative mix
- Group 2 . . 9 cells with 5% asbestos fibers in negative mix
9 cells with 10% asbestos fibers in negative mix
9 cells with 15% asbestos fibers in negative mix
- Group 3 . . . 9 cells with 5% zinc fibers in negative mix
9 cells with 10% zinc fibers in negative mix
9 cells with 15% zinc fibers in negative mix

Included are three control cells. All cells were activated in 50% KOH and were cycled at 60% depth-of-discharge. Figure 1 shows the initial capacity of these cells. Figure 2 shows the number of cycles obtained by Group 1 cells. Figures 3 and 4 show the number of cycles obtained by the cells in Groups 2 and 3 respectively. These cells failed by loss of negative plate capacity.

In an effort to increase overall cycle life under 60% DOD, a cell design utilizing more and thinner plates per cell to afford a lower current density per plate is under study.

Twenty-seven 25 a.h. cells containing 19 plates were constructed with asbestos fibers as follows:

- 9 cells with .5% asbestos in the negative mix
- 9 cells with 1% asbestos in the negative mix
- 9 cells with 1.5% asbestos in the negative mix
- 3 cells as controls.

These cells failed at 73 cycles. The control cells failed at 157 cycles.

The cause of failure was loss of capacity due to dry plates. This condition occurs because of pack tightness when four layers of separation are used. Additional cells in the following paragraphs were tested using three and four layers of separation to test whether the dry condition in the cells could be eliminated by going to fewer separator layers.

Figures 5 through 13 are photomicrographs of the negative plates containing percentages of these binders at indicated cycles.

D. Particle Size and Morphology of Zinc Oxides

Various types of oxides have been received from the New Jersey Zinc Company. Work on these oxides will be started shortly when the cell design is finalized at 60% DOD.

E. Zinc Electrode Fabrication Techniques

Twenty-five a.h. cells containing 21 plates and four layers of FSC separation were constructed and tested with the following percentages of XX-601 zinc oxides (acicular) as follows:

- 9 cells with 5% XX-601 in the negative mix
- 9 cells with 10% XX-601 in the negative mix
- 9 cells as controls.

Additional cells containing 17 plates and four layers of FSC separation were constructed and tested for the following percentages of XX-4 zinc oxide (acicular) as follows:

- 3 cells with 2% XX-4 in the negative mix
- 3 cells with 5% XX-4 in the negative mix
- 3 cells with 10% XX-4 in the negative mix
- 3 cells as controls.

The cells containing the XX-601 acicular zinc oxide gave 25 a.h. initial capacity and failed at 77 cycles, including the control cells. The cause of failure was due to dry plates because of pack tightness.

The cells containing the XX-4 acicular zinc oxide gave 22 a.h. initial capacity and failed at 157 cycles, including the control cells. The cause of failure was loss of negative plate capacity.

Figures 14 to 19 show the cross-sectional photomicrographs of the negative plates at the percentages of the acicular zinc oxides and the number of cycles obtained at 60% DOD.

Twenty-one additional 25 a.h. cells containing 21 plates were constructed with varying percentages of zinc carbonate and zinc sulfate in the negative plate mix as follows:

- 3 cells as controls
- 3 cells with 2% $ZnCO_3$ in the negative mix
- 3 cells with 5% $ZnCO_3$ in the negative mix
- 3 cells with 10% $ZnCO_3$ in the negative mix
- 3 cells with 2% $ZnSO_4$ in the negative mix
- 3 cells with 5% $ZnSO_4$ in the negative mix
- 3 cells with 10% $ZnSO_4$ in the negative mix

These cells delivered 33 a.h. to 37 a.h. initial capacity. Figure 20 shows the number of cycles obtained by these cells. These cells failed due to loss of negative plate capacity. There were also heavy deposits of Zn trees on the edges of the elements.

The addition of $ZnSO_4$ appears to aid the cycle ability of the negative plate in this series at 60% DOD.

The photomicrographs of these negative plates are under preparation at this time.

F. Influence of Membrane Separator Characteristics

The First Quarterly Report prepared by the Whittaker Corporation is enclosed.

I. Sizes of Zincate Ion and Soluble Silver Species in KOH

In an attempt to achieve a better understanding of concentrated KOH solutions, available data from the literature have been treated as discussed herein. The main objective of this work is to achieve a value for ion sizes of K^+ and OH^- in concentrated solutions of battery strength. The work reported herein is our first approach to the problem and is incomplete insofar as data for ions have not yet been achieved, except in terms of upper and lower limits; however, data existing in the literature can be treated to obtain molecular volumes for hydrated KOH in battery strength solutions.

Partial Molal Volumes

As a first step in the procedure, the density data* for KOH solutions up to 50% by weight (68°F.) were used to calculate the volume of solutions containing 1000 grams of water. The data are shown in Table I.

TABLE I

Volumes of KOH Solutions (68°F.)

Weight % KOH	Density	Volumes of Sol- utions Containing 1000 gm. H ₂ O (c.c.)	Weight KOH Grams	Molality n ₂
0	0.997	1003	0	0
2	1.016	1004	20	0.36
6	1.053	1010	65	1.16
10	1.090	1022	112	2.00
16	1.147	1037	190	3.39
24	1.226	1074	317	5.65
30	1.288	1110	430	7.66
40	1.396	1193	668	11.9
50	1.512	1322	1000	17.8

*JACS, Apr. 1941, p. 1088

From these data, the solution volume may be plotted against the molality, as in Figure 22. The tangent to the curve at any value of molality provides data for the calculation* of the partial molar volume. As an example, from the tangent at 40% by weight KOH, the volume per mole of KOH in solution is calculated to be 20.5 c.c. This may be compared with 27.4 c.c. calculated from the handbook value of 2.044 gm per c.c. for the density of solid KOH.

From the molar volume, the volume per molecule of KOH in solution may be calculated using Avagadro's number

$$\frac{20.5}{6.023 \times 10^{23}} = 3.41 \times 10^{-23} \text{ c.c.}$$

or

$$3.41 \times 10^{-23} \times 10^{24} = 34.1 \text{ cubic Angstroms.}$$

If the molecule is treated as a sphere the molecular diameter is calculated to be

$$d^3 = \frac{6 \times 34.1}{\pi} = 65$$

$$d = 4 \text{ \AA}^{\circ}$$

On this basis, the diameter of either the K^+ ion or the OH^- ion would be less than 4 \AA° .

From the shape of the curve, it is evident that the molar volume of the KOH gets progressively less as the concentration of solution decreases. Thus, at $n_2 = 2$ (10% by weight KOH), the molar volume is calculated from the tangent to be 12 c.c./mole. Evidently KOH solutions are quite non-ideal, and the molecular volumes are far from being additive. Just how far they are from being additive is described in Figure 23 where volume per mole for KOH solutions is plotted against mole fraction of KOH. These data were calculated from Table I.

*See "Textbook of Physical Chemistry," Glasstone, 2nd Ed. p. 239. D. VanNostrand Co., Inc., 1946.

What this means, of course, is that the ions from dissolved KOH are more-or-less hydrated in solution. As a consequence, the molecular volume and diameter previously calculated for KOH in 40% solution may be considered to be effective values for KOH stripped of waters of hydration, and, therefore, not representative of the real situation in solution. While Figure 23 says that there is a good deal of solute-solvent interaction, the data of the figure do not provide quantitative means of determining how much water is tied up by dissolved KOH.

Degree of KOH Hydration

A thorough review of the literature has not yet been made, but it is speculated that a dearth of data aimed at determining degree of hydration in battery strength electrolytes is apt to be found. At any rate, a treatment of existing literature data is made herein, which is believed to be novel, although no claim is made for its scientific rectitude.

The concept and treatment of data are very simple.

Determination of molecular weights from freezing point depression, boiling point elevation, vapor pressure reduction, etc. are all commonly used techniques, and any standard elementary physical chemistry text provides the theoretical basis for making such determinations. Furthermore, the same texts discuss solutions of strong electrolytes where 100% ionization is assumed to be the case. The major problem seems to be that such experimental data are good only for relatively dilute solutions (1 to 2 molal or less).

When freezing point depression data, boiling point elevation data, and vapor pressure lowering data for KOH solutions are examined, it is apparent that the quantities involved become substantially larger than those which can be calculated on the basis of the simple theory, assuming 100% ionization, as concentration increases beyond 1 or 2 molal. It is suggested hereby that this result occurs simply because of the hydration of ions (and/or,

molecules), and that comparison of the actual data with that calculated as theoretical based on 100% ionization can provide a means of determining the extent of hydration. What this means is this: because of hydration the water of hydration becomes a component of the solute* and, consequently, the real concentration of solute becomes appreciably larger than that calculated from the straight molal quantities of each component originally added to make up the solution.

We may choose the vapor pressure lowering relationship to illustrate the treatment of data. In Figure 24 are shown the measured values of vapor pressure of water for solutions of KOH up to 50% by weight at 68° F. (International Critical Tables, Vol. III, p. 373). On the same graph are shown calculated values of the vapor pressure which should result based, simply, on a molal lowering of 0.62 mm/mole. (0.31 is taken as the molal lowering for a non-ionized solute which obeys Raoult's law. See "Physical Chemistry for Colleges," Millard, 6th Ed., p. 183, McGraw-Hill, 1946.)

The tie lines drawn indicate that a 4 molal solution behaves like a theoretical 5.8 molal solution; a 6 molal solution behaves like a theoretical 9.4 molal solution; an 8 molal solution behaves like 13.1 molal solution, and so forth.

Now, a 5.8 molal solution contains 55.6 moles of water in the ratio 5.8/55.6, so the 4 molal solution behaves as though it contains water in the same ratio

$$\frac{4.0}{x} = \frac{5.8}{55.6}$$
$$x = 38.4$$

But, inasmuch as the 4 molal solution actually contains 55.6 moles of water, then $55.6 - 38.4 = 17.2$ moles of water have become part

*See for Example: "Ionic Sizes," Stern and Anis, Chem. Rev. 52, Feb. 1959, p. 23.

of the solute as water of hydration. Therefore 17.2 moles of water are associated with 4 moles of KOH for a hydration number of 4.3. In similar fashion a hydration number can be calculated for each concentration of KOH and the curve described in Figure 25 is obtained. This curve says that the number of moles of water associated with one mole of KOH falls off sharply as concentration is increased.

Now we are in a position to calculate the size of the hydrated molecule. Using a 40% by weight solution again, from Figure 25 it is seen that 1.67 moles of water are tied up with 1 mole of KOH. Because there are 11.9 moles of KOH in a 40% solution, 19.9 moles of water are hydrated, leaving 35.7 moles of solvent water. If it is assumed that solvent water has the same specific volume as pure water, then the volume of solvent water is

$$35.7 \times 18.1 = 646 \text{ c.c.}$$

But, from Figure 22 an 11.9 molal solution containing 1000 grams of water has a volume of 1190 c.c. Therefore, the volume of hydrated KOH is

$$1190 - 646 = 544 \text{ c.c.}$$

or

$$544/11.9 = 45.6 \text{ c.c./mole.}$$

The value of 45.6 c.c./mole may be compared with the additive value of 57.6 calculated from the molar volume of solid KOH and that for 1.67 moles of pure water.

Again, using Avagadro's number, the volume per hydrated molecule for KOH in a 40% solution is

$$\frac{45.6}{6.023 \times 10^{23}} = 7.57 \times 10^{-23} \text{ c.c.}$$

or

$$7.57 \times 10^{-23} \times 10^{24} = 75.7 \text{ cubic Angstroms.}$$

If the hydrated molecule is treated as a sphere, the molecular diameter is calculated to be 5.3 Å. For a 4 molal solution

(hydration number 4.3), the volume per molecule is calculated to be 146 cubic Angstroms and the spherical diameter to be 6.5 \AA . On this basis, the diameter of either the hydrated K^+ ion or the hydrated OH^- ion would be less than 6.5 \AA for the latter solution.

Derived Data

From Figure 25 a very interesting plot can be made up. From the molality and the hydration number, the total moles of water tied up as water of hydration can be calculated. The result is shown in Figure 26 for solutions containing 1000 grams of water (55.6 moles). It is interesting that this curve goes through a maximum around 8 molal (32% by weight KOH). The conductivity is plotted on the same chart for comparison. Obviously, similar maxima would occur if these plots were made on a molar basis, rather than on a molal basis.

It is suggested that this result, namely a maximum in quantity of bound water, as well as the sharp falling off of the hydration number as concentration increases, may be due to the same overall effect: a sharp increase in the degree of ion association between K^+ and OH^- as concentration increases above about 20 - 25% by weight. Thus, as ions of opposite charge come more and more within one another's influence, water of hydration might not only be physically shoved away but also lessened in quantity because of a reduced effective ionic charge. The decreased conductivity might be, in part, due to an actual reduction in the effective number of ionic carriers, as well as to increased viscosity.

If the latter description is true, i.e. ion-ion association, then the calculated curve in Figure 24 would fall off less sharply than shown at the higher concentrations and the degree of hydration would have to be recalculated correcting for the extent of ion-ion association. It seems possible that some estimate of ion-ion

association could be obtained from the conductivity data, and an attempt will be made to work this out for the next report.

Conclusion

A simple theory is presented for the shape of vapor pressure, freezing point, and boiling point curves for KOH solutions as a function of concentration, and their variation from theoretical curves based on 100% ionic dissociation. Available literature data enable the calculation of extent of molecular hydration and limiting sizes for hydrated molecules of KOH. It is likely that ionic association will necessitate a correction to the calculated values of extent of hydration, in the more concentrated solutions, which would have the effect of increasing the calculated values of extent of hydration.

N. Surfactant Tests

Ninety 25 a.h. cells containing 21 plates and three layers of FSC separation were constructed containing the following surfactants and percentages in the negative plate mix:

- 9 cells with .15% EC-420
- 9 cells with .60% EC-420
- 9 cells with 1% EC-420
- 9 cells with .15% EC-720
- 9 cells with .60% EC-720
- 9 cells with 1% EC-720
- 9 cells with .15% EC-840
- 9 cells with .60% EC-840
- 9 cells with 1% EC-840
- 9 cells with .5% EC-610 as Controls.

These cells delivered between 28 and 39 a.h. initial capacity. Figure 21 shows the number of cycles obtained by each surfactant tested. The cause of failure was due to loss of negative plate capacity in the case of EC-720 and EC-420. There is no apparent cycle life improvement for the various percentages of each individual surfactant. The cause of failure in surfactant EC-840 was massive short circuiting. In all cases in the majority of the cells tested, heavy treeing of the zinc material was evident along the edge of the elements. The control cells are still cycling.

The photomicrographs of the negative plates are under preparation and will be furnished in the next quarterly report.

It is thought that the excessive treeing experienced in this and earlier tests is in some way related to the use of thin plates in this cell design. The standard 15 plate cell design did not appear to promote this condition.

Additional cells are under test with varying plate numbers, and shortly a cell design will be finalized for use in this program which will best utilize the 60% DOD regime.

III. Summary

The use of FSC and asbestos fibers do not improve the cycle life of the cell at 60% depth-of-discharge over the control cells. The use of zinc fibers shows some improvement, but this is because additional zinc is added to the cell. Additional organic fibers are to be tested.

Zinc sulfate seems to improve cycle life, and further tests with increased percentages will be made.

The surfactants EC-720, EC-840, and EC-420 do not improve cycle life over the standard EC-610 at 60% depth-of-discharge. Tests are to continue using some tertiary alcohols and carbowaxes to determine what structure of the surfactant is responsible for the improved negative electrode performance.

On the basis of literature data for density of KOH solutions and a novel method of treatment of vapor pressure lowering data ranges of molecular size can be calculated in terms of extent of hydration.

DISTRIBUTION LIST

<u>NR CYS</u>	<u>ACTIVITIES AT WPAFB</u>	<u>NR CYS</u>	<u>OTHER DOD ACTIVITIES (Cont'd)</u>
1	SEPR		<u>Air Force</u>
1	SEPRR	1	AFCRL (CRZK, Mr. Doherty) I. G. Hanscom Field Bedford, Mass.
1	APE		
1	APIP	1	SSD (SSTRE, Maj. Iller) AF Unit Post Office Los Angeles, Calif. 90045
2	APIP-2	20	Defense Documentation Center Cameron Station Alexandria, Virginia 22314
<u>OTHER DEPT. OF DEFENSE ACTIVITIES</u>			
<u>Army</u>			
1	Dr. Adolf Fischback (Chairman) Special Purpose Battery Branch Power Sources Division U.S. Army Signal R&D Laboratory Attn: SIGRA/SL-PSS Ft. Monmouth, New Jersey	1	<u>NATIONAL AERONAUTICS AND SPACE ADMINISTRATION</u> NASA Attn: Mr. Ernst M. Cohn Code RNW Washington, D. C. 20546
1	OASD (R&E), Room 3E-1065 The Pentagon Attn: Technical Library Washington 25, D. C.	1	NASA Lewis Research Center Attn: Dr. Louis Rosenblum 21000 Brookpark Road Cleveland 35, Ohio
1	Commanding Officer Diamond Ordnance Fuze Laboratory Attn: Library, Room 211 Building 92 Washington 25, D. C.	1	NASA Marshall Space Flight Center Attn: Mr. Richard Boehme Huntsville, Alabama
1	U.S. Army Signal R&D Laboratory Attn: Mr. Paul Rappaport Ft. Monmouth, New Jersey	1	NASA Lewis Research Center Attn: Harvey Schwartz 21000 Brookpark Road Cleveland 35, Ohio
<u>Navy</u>			
1	Mr. P. Cole (Code WB) Naval Ordnance Laboratory Silver Spring, Maryland	2	Scientific and Technical Information Facility Attn: NASA Representative (SAK/DL) P. O. Box 5700 Bethesda, Maryland 20014

DISTRIBUTION LIST (Continued)

Navy

1 Mr. W. H. Fox
Office of Naval Research
(Code 425)
Department of the Navy
Washington 25, D. C.

1 Naval Ordnance Laboratory
Attn: W. C. Spindler
Corona, California

NON-GOVT. INDIVIDUALS AND AGENCIES

1 Yardney Electric Corporation
Attn: Dr. George Dalin
40-52 Leonard Street
New York 13, New York

1 Gulton Industries, Inc.
Attn: R. C. Shair
212 Durham Avenue
Metuchen, New Jersey

NON-GOVT. INDIVIDUALS AND AGENCIES

1 Dr. Arthur Fleischer
466 S. Center Street
Orange, New Jersey

1 P. R. Mallory & Co., Inc.
Laboratory for Physical Science
Attn: Mr. F. J. Cocca
Northwest Industrial Park
Burlington, Massachusetts

1 Dr. T. P. Dirkse
Department of Chemistry
Calvin College
Grand Rapids, Michigan 49506

1 Lockheed Missiles & Space Co.
Attn: Dr. J. E. Chilton
Department 52-30
3251 Hanover Street
Palo Alto, California

1 Aerospace Corporation
P. O. Box 95085
Los Angeles, California 90045

1 Jet Propulsion Laboratory
California Institute of
Technology
4800 Oak Grove Drive
Pasadena, California 91103

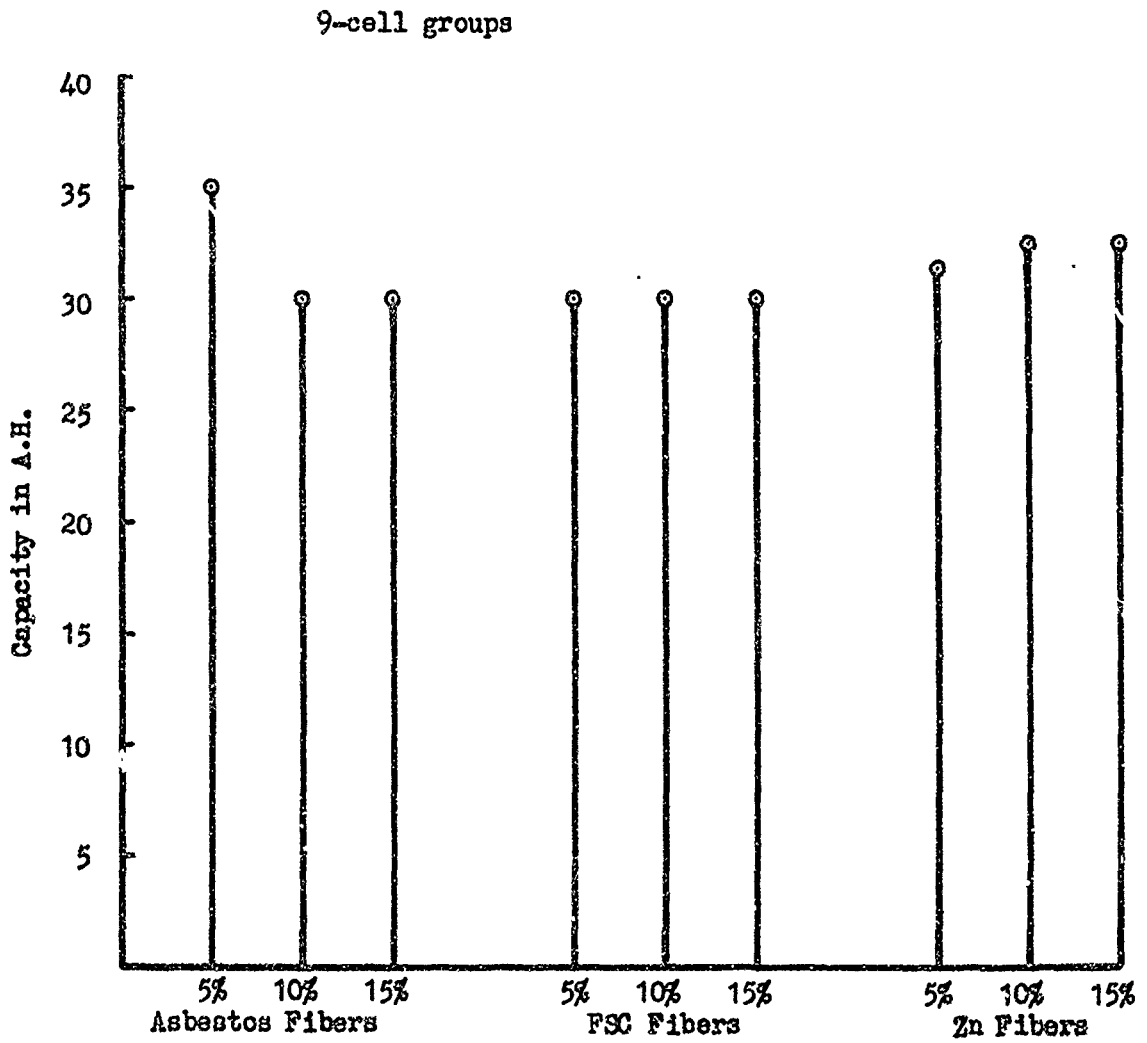


Figure 1. Initial Capacity of Cells Containing Various Fibers in Negative Plates

All cells cycled at 60% DOD

C = control cells

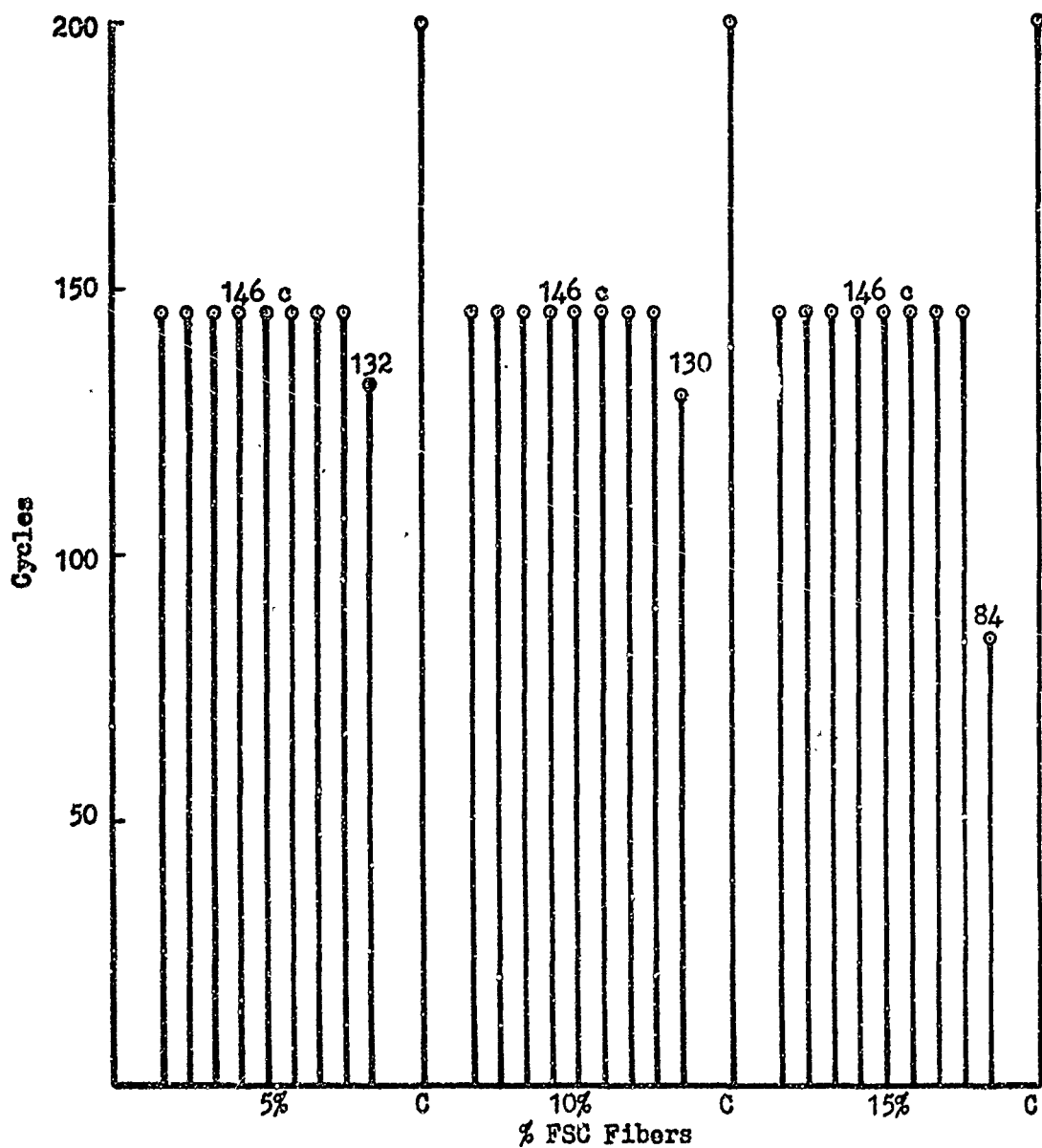


Figure 2. Number of Cycles Obtained by Cells in Group 1

All cells cycled at 60% DOD

C = control cells

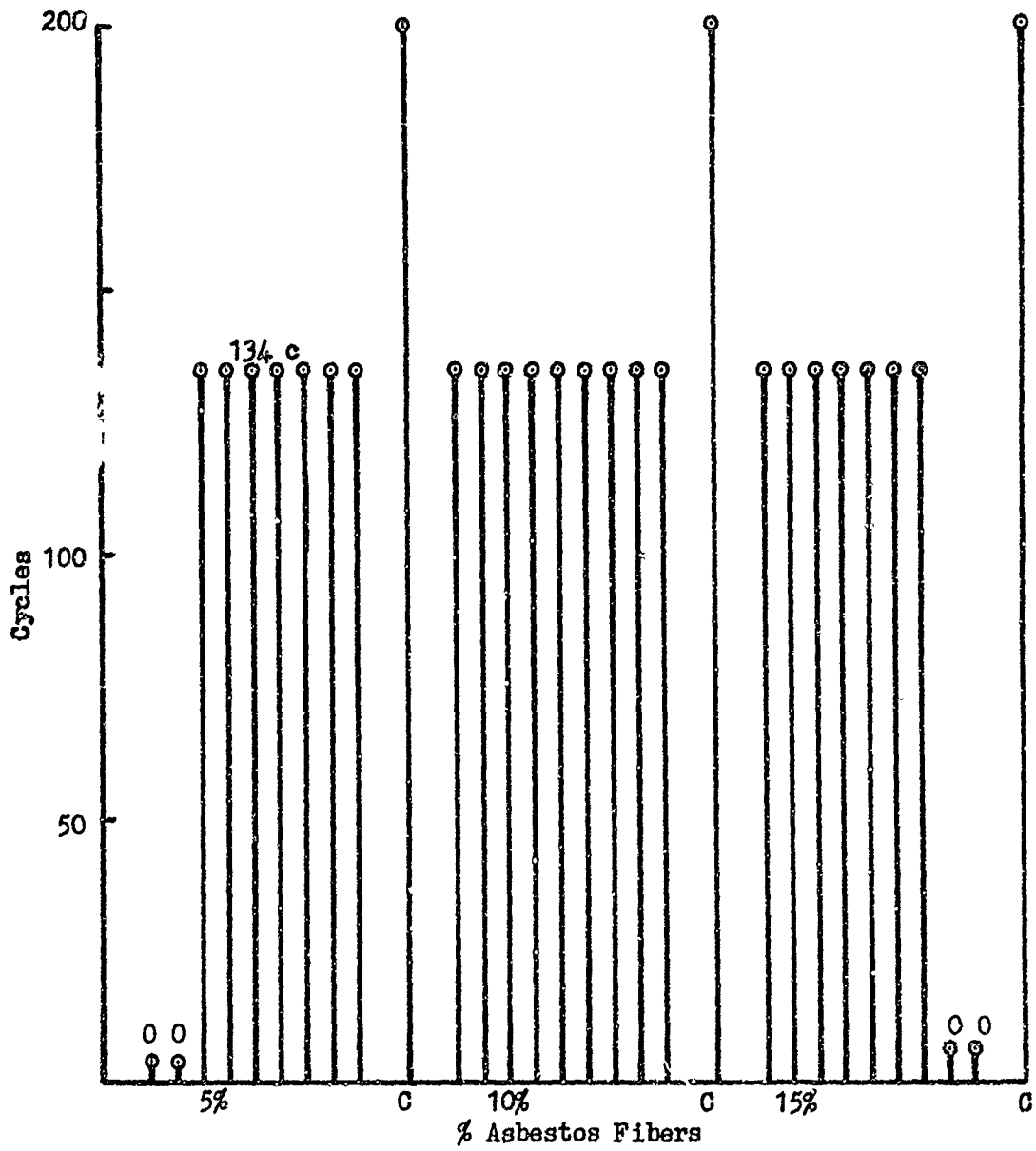


Figure 3. Number of Cycles Obtained by Cells in Group 2

All cells cycled at 60% DOD

C = control cells

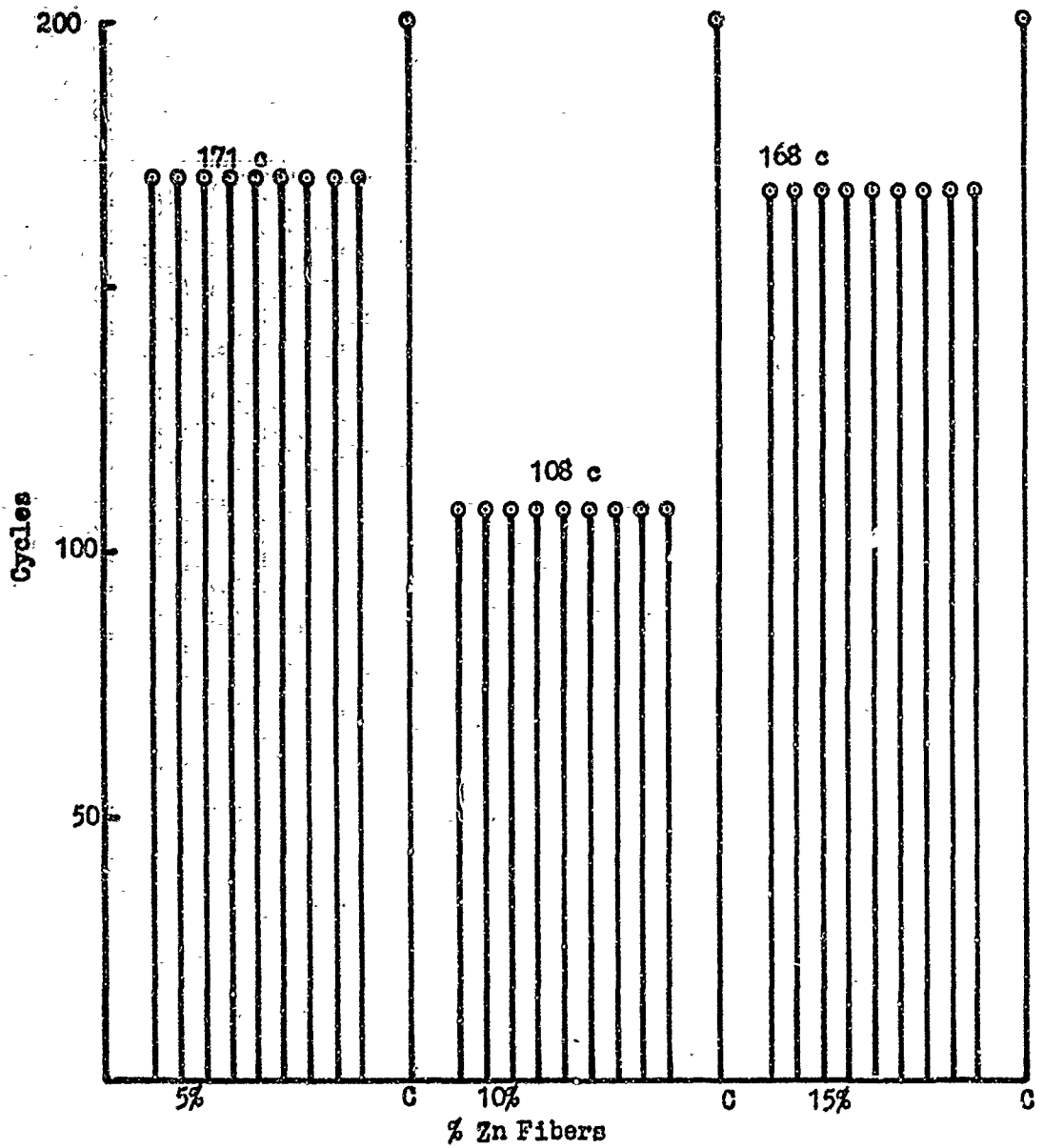


Figure 4. Number of Cycles Obtained by Cells in Group 3

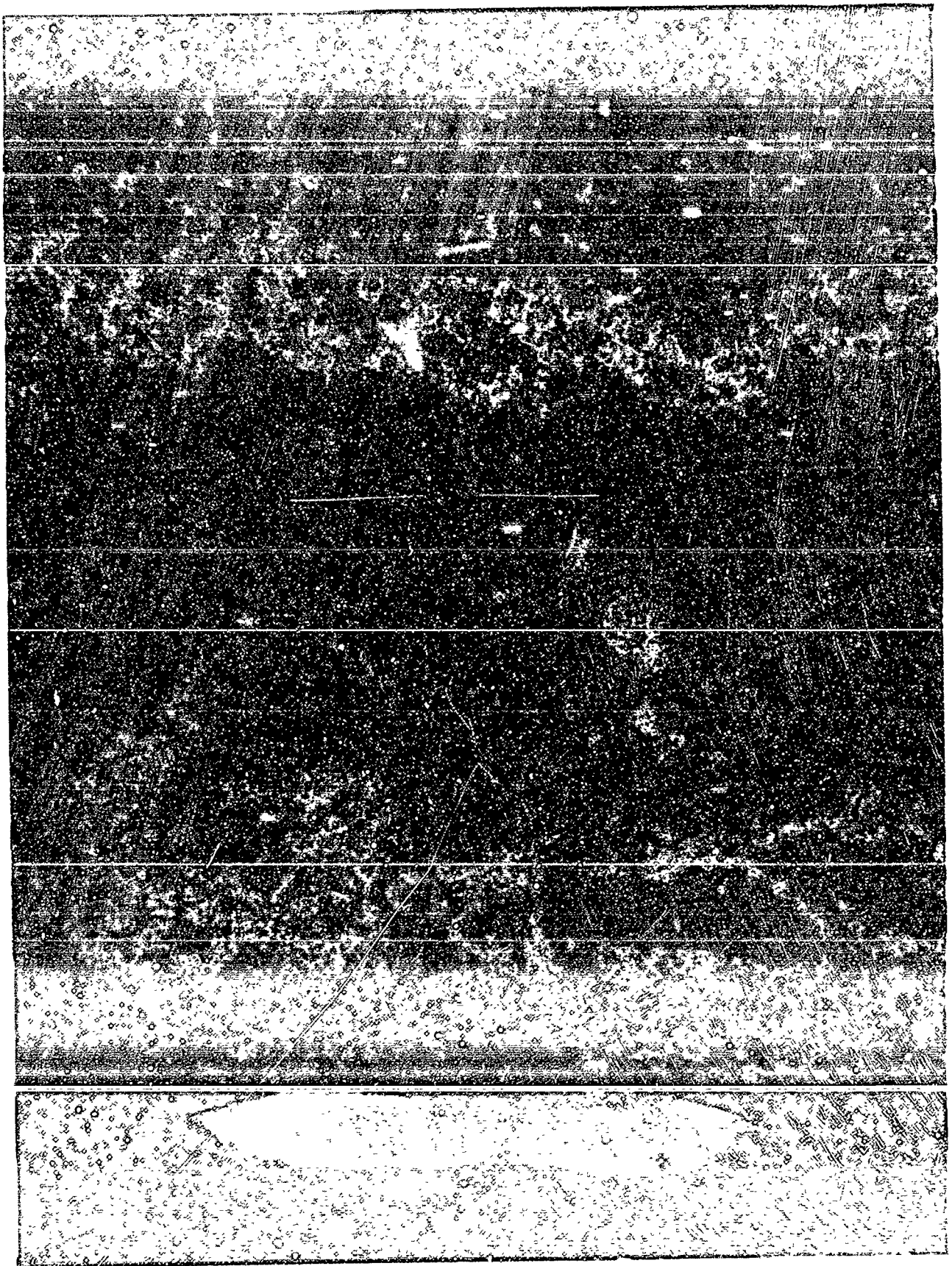


Figure 5. Negative Plate Containing 5% FSC Fibers at 146 Cycles

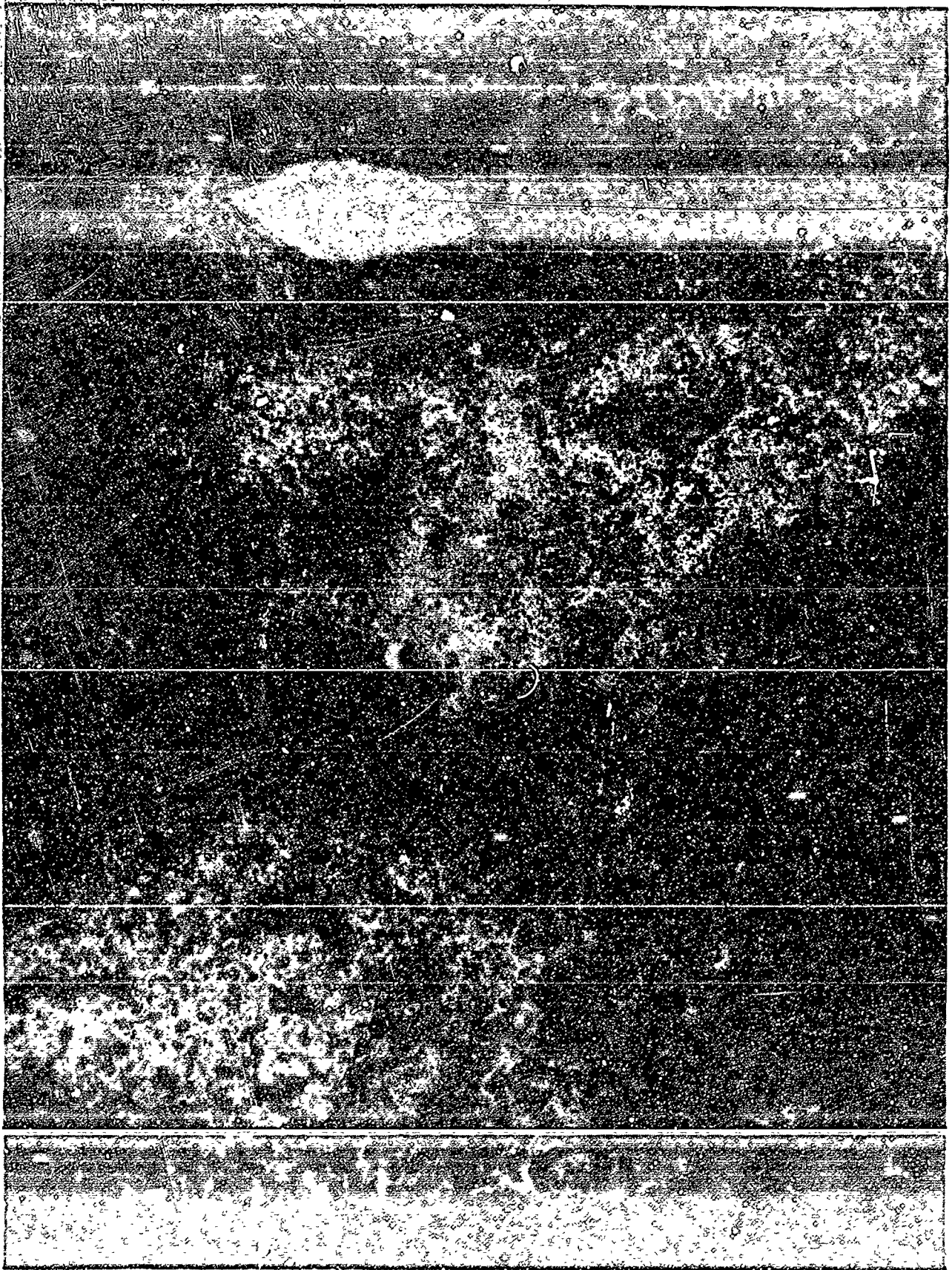


Figure 6. Negative Plate Containing 10% FSC Fibers at 146 Cycles



Figure 7. Negative Plate Containing 15% FSC Fibers at 146 Cycles

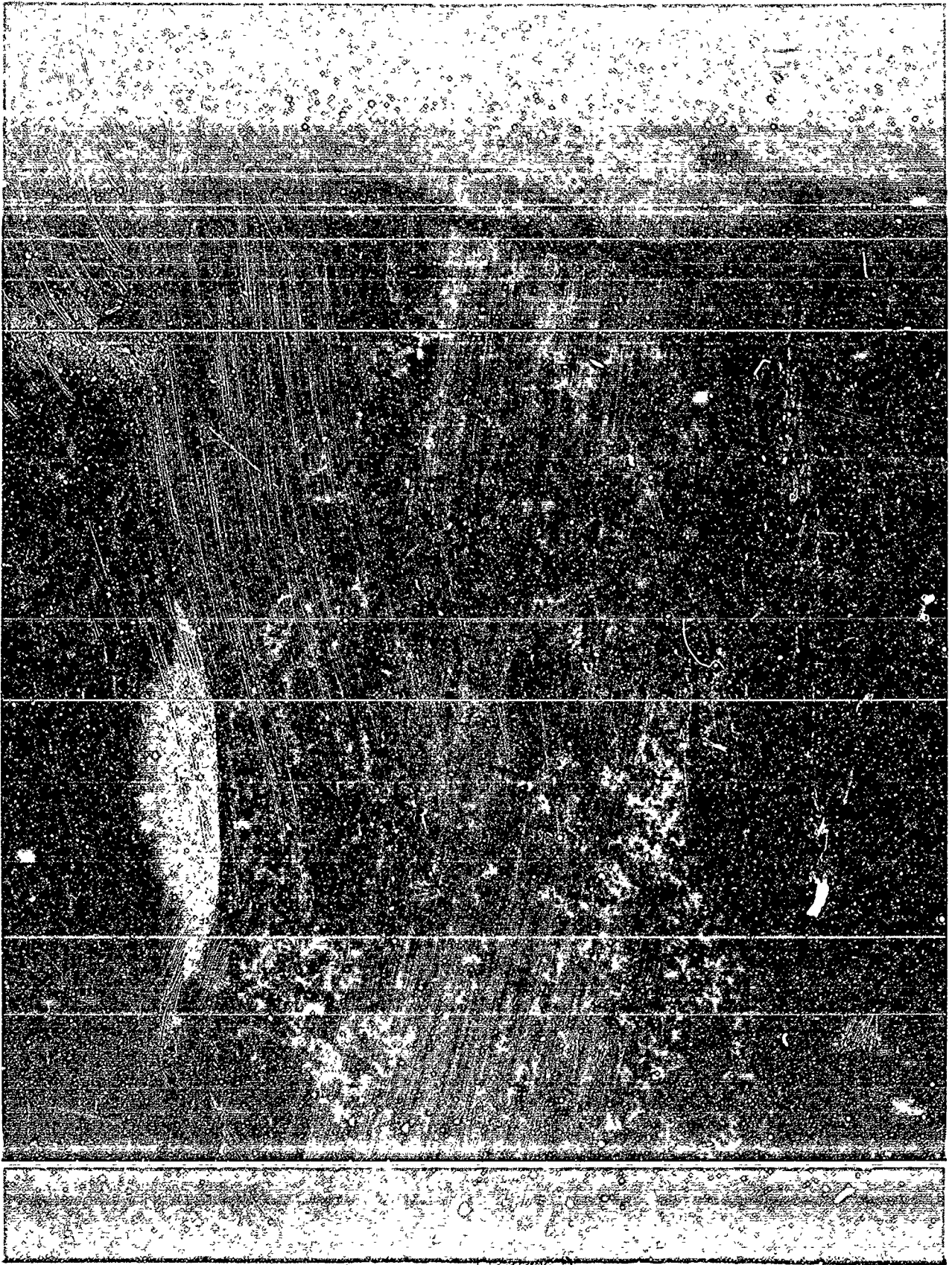


Figure 8. Negative Plate Containing 5% Asbestos Fibers at 134 Cycles

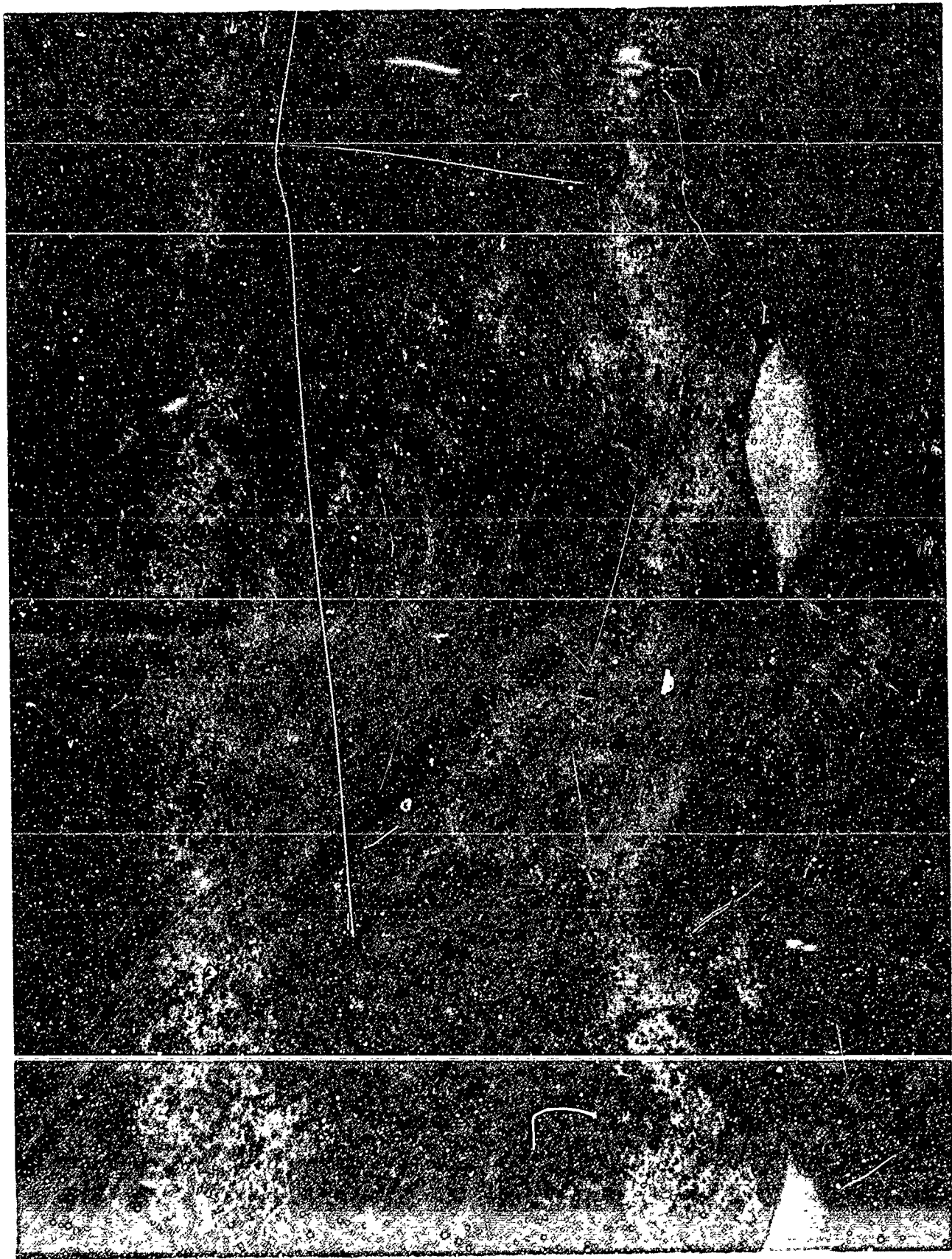


Figure 9. Negative Plate Containing 10% Asbestos Fibers at 134 Cycles



Figure 10. Negative Plate Containing 15% Asbestos Fibers
at 134 Cycles

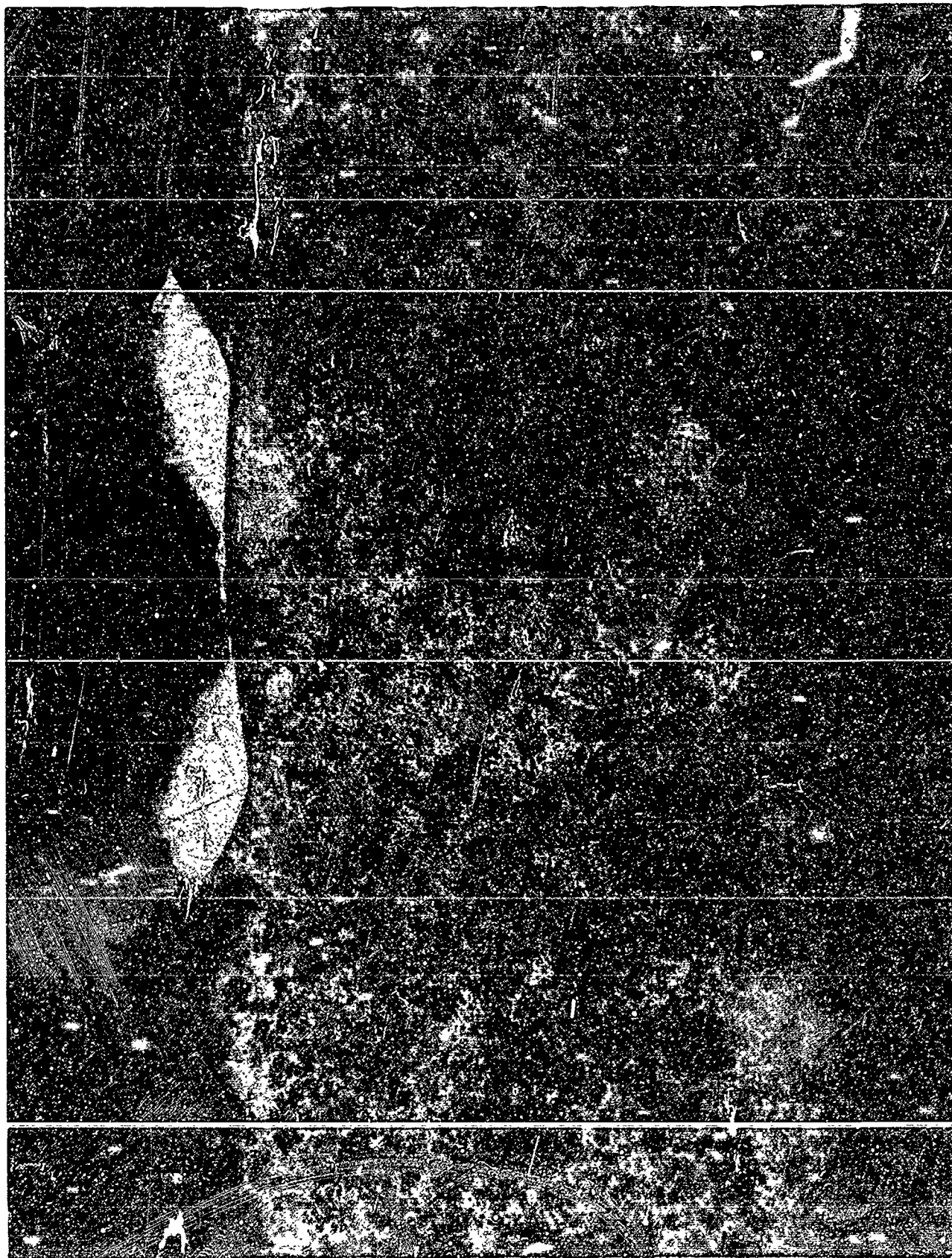


Figure 11. Negative Plate Containing 5% Zinc Fibers at 171 Cycles

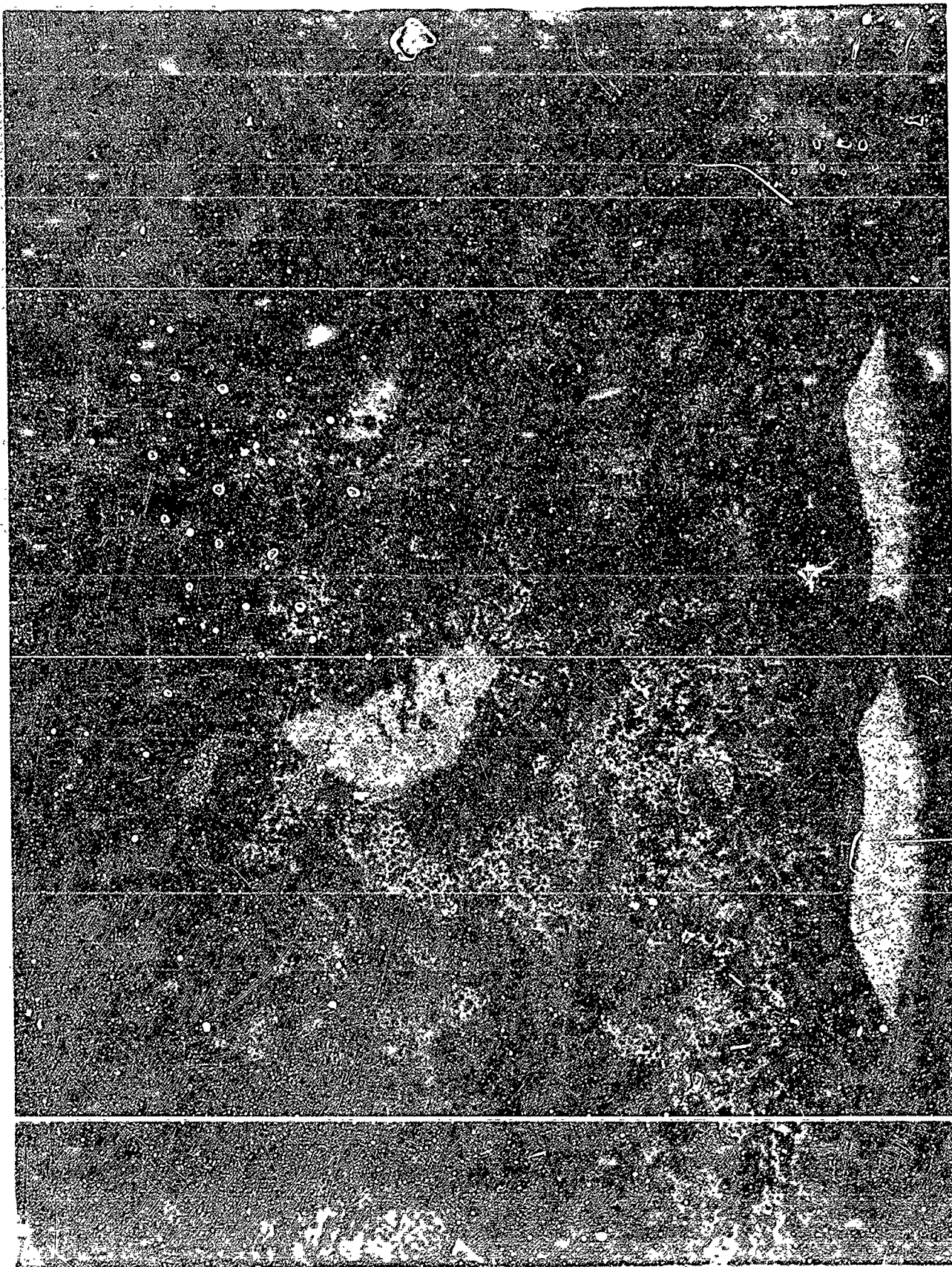


Figure 12. Negative Plate Containing 10% Zinc Fibers at 108 Cycles

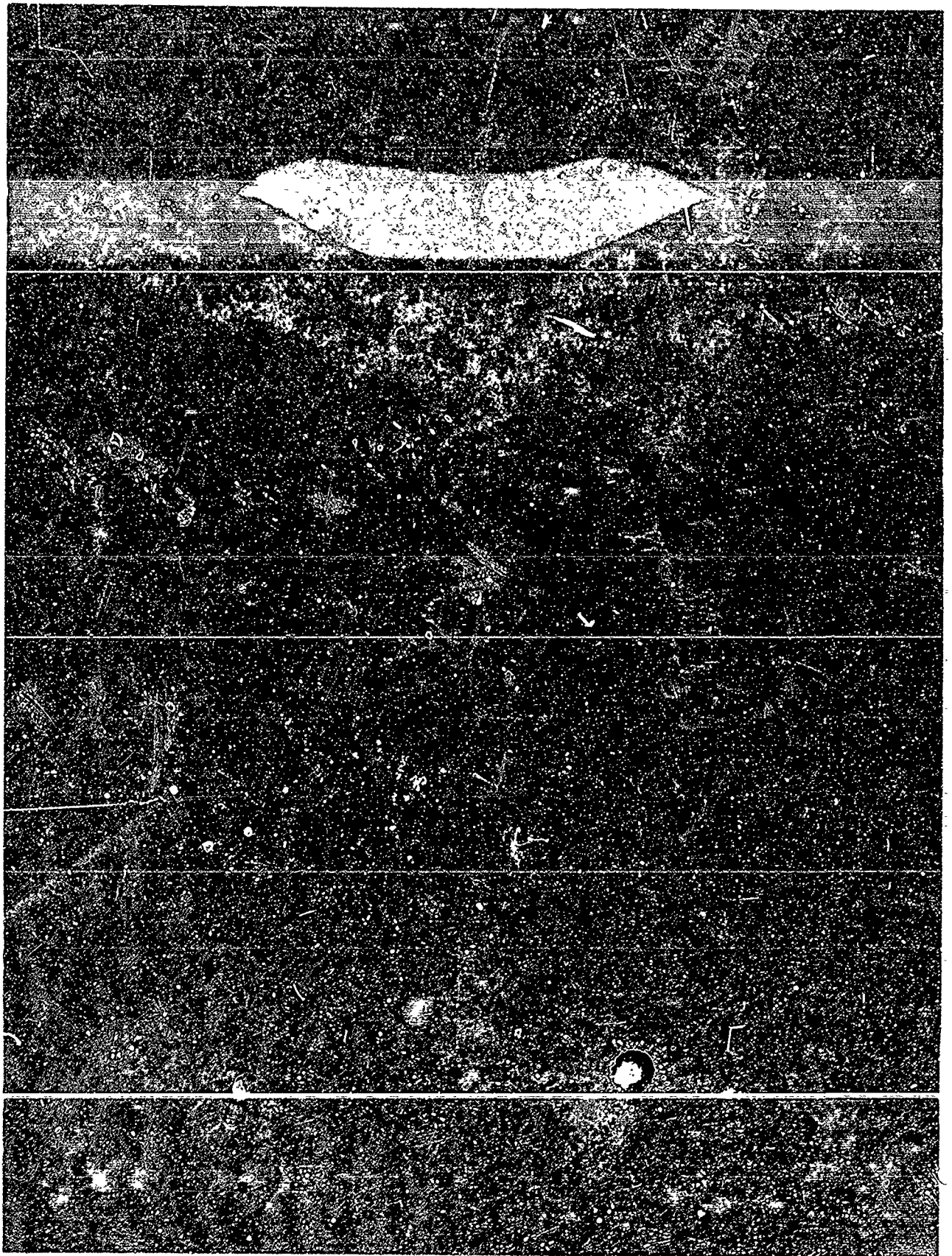


Figure 13. Negative Plate Containing 15% Zinc Fibers at 168 Cycles

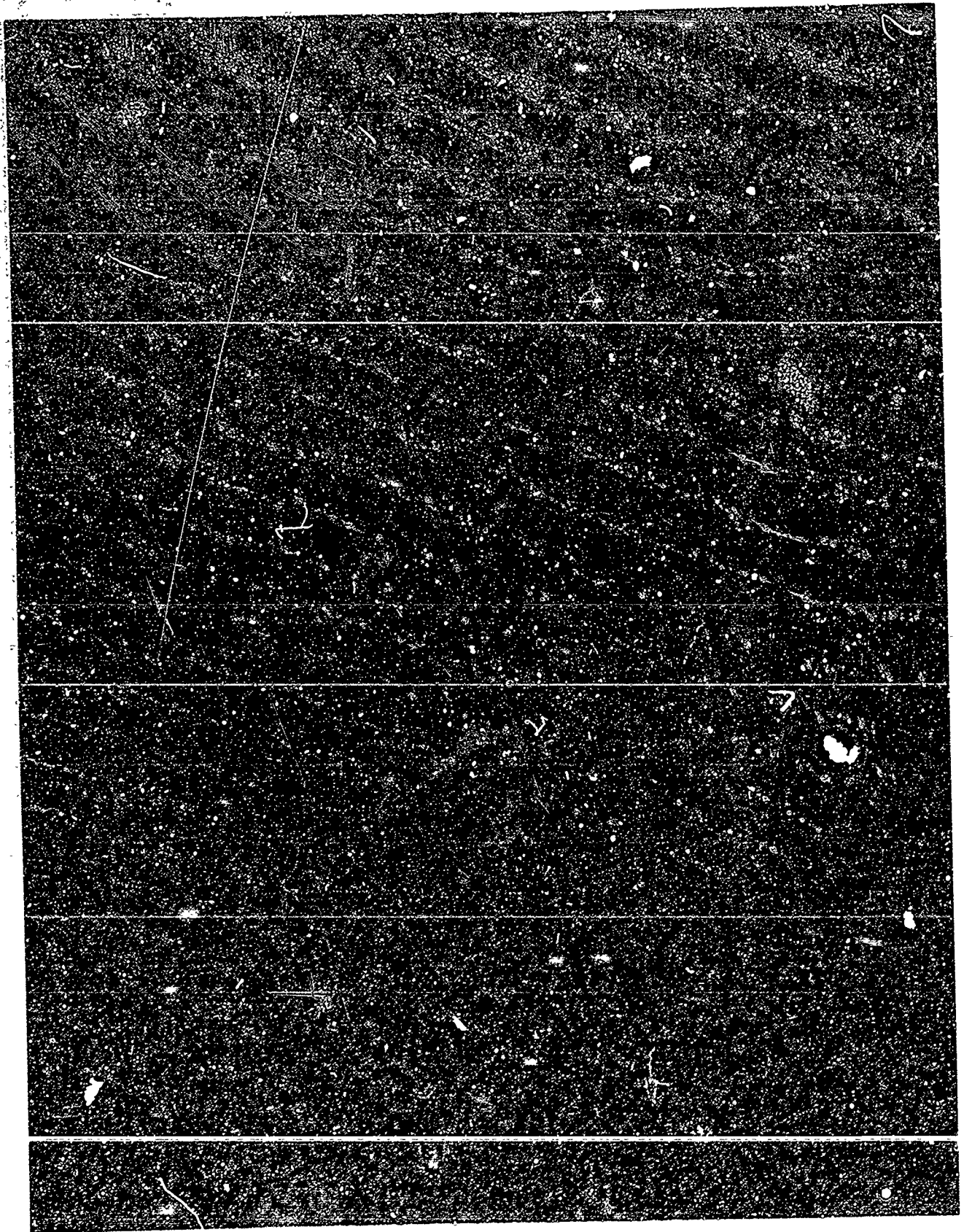


Figure 14. Negative Plate of Control Cell for XX-601 and XX-4
Acicular Oxides at 77 Cycles

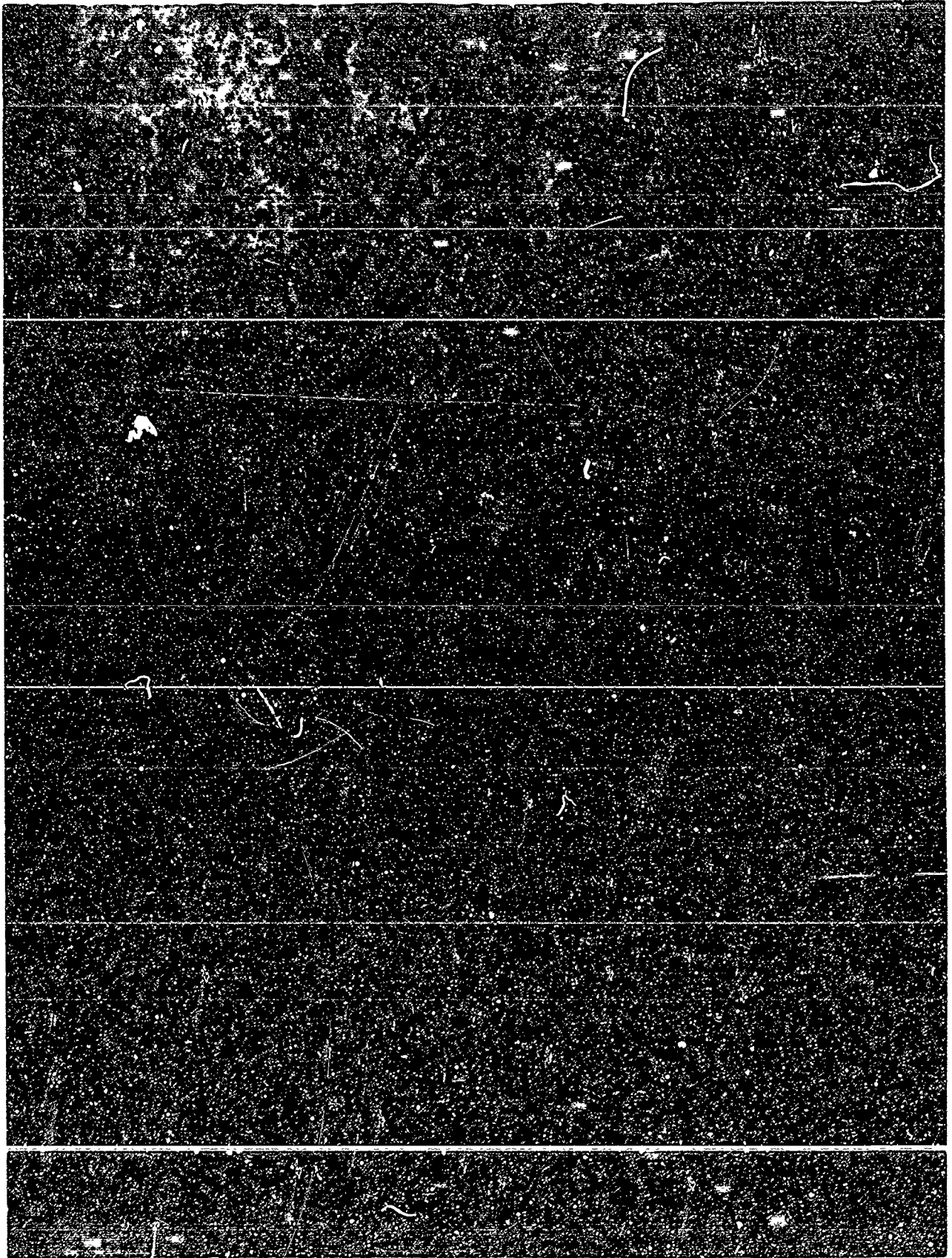


Figure 15. Negative Plate Containing 5% XX-601 ZnO at 77 Cycles

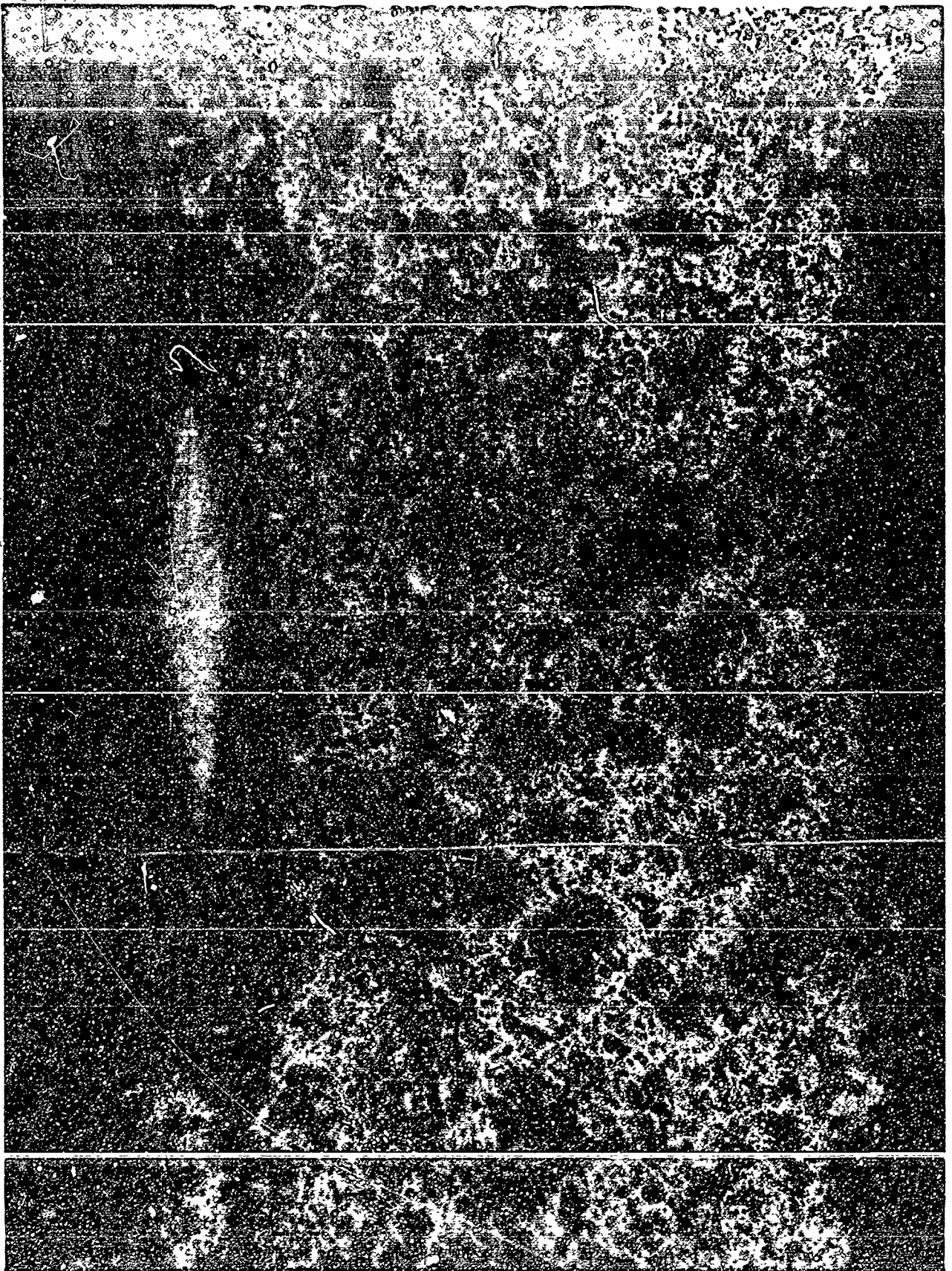


Figure 16. Negative Plate Containing 10% XX-601 ZnO at 77 Cycles

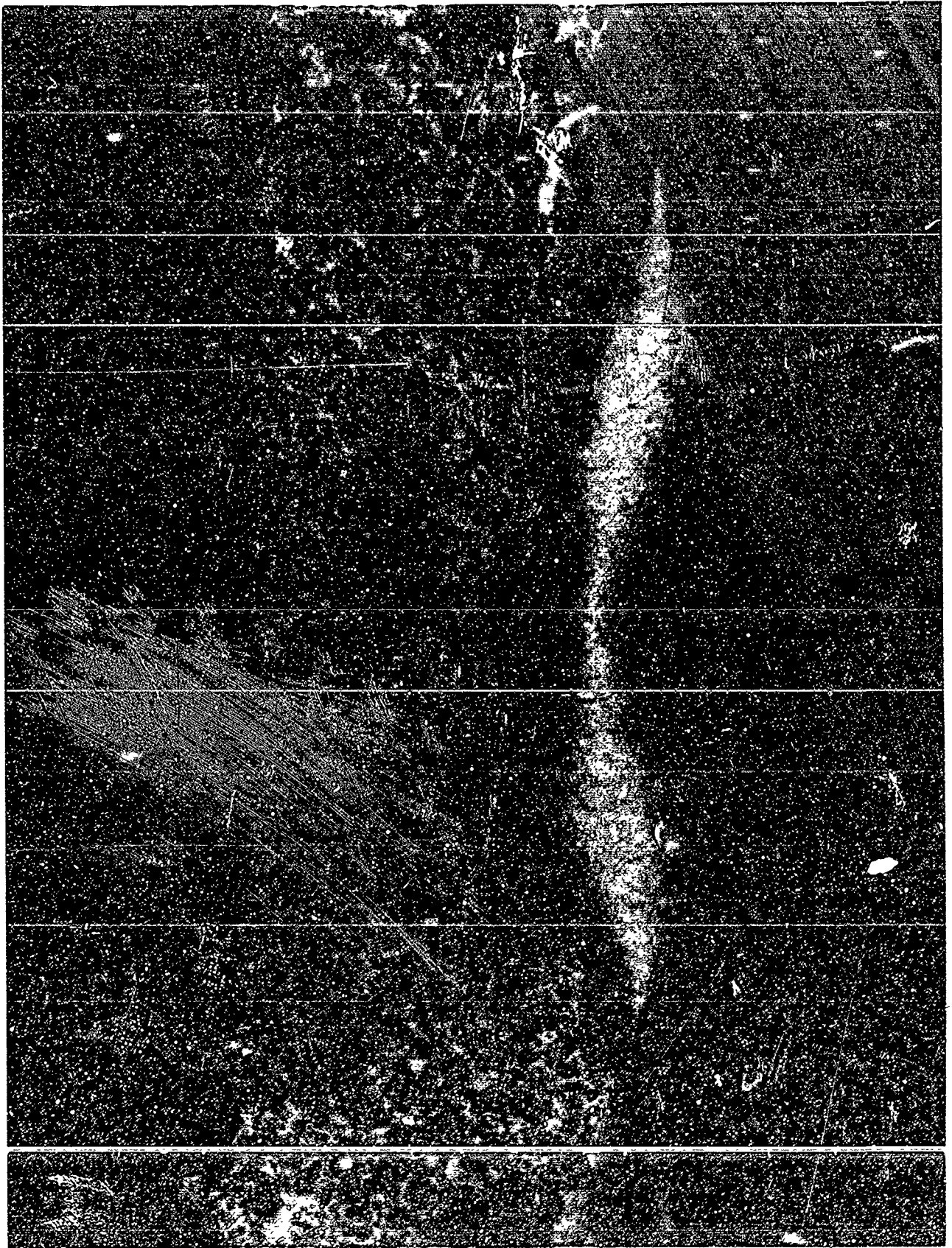


Figure 17. Negative Plate Containing 2% XX-601 ZnO at 77 Cycles

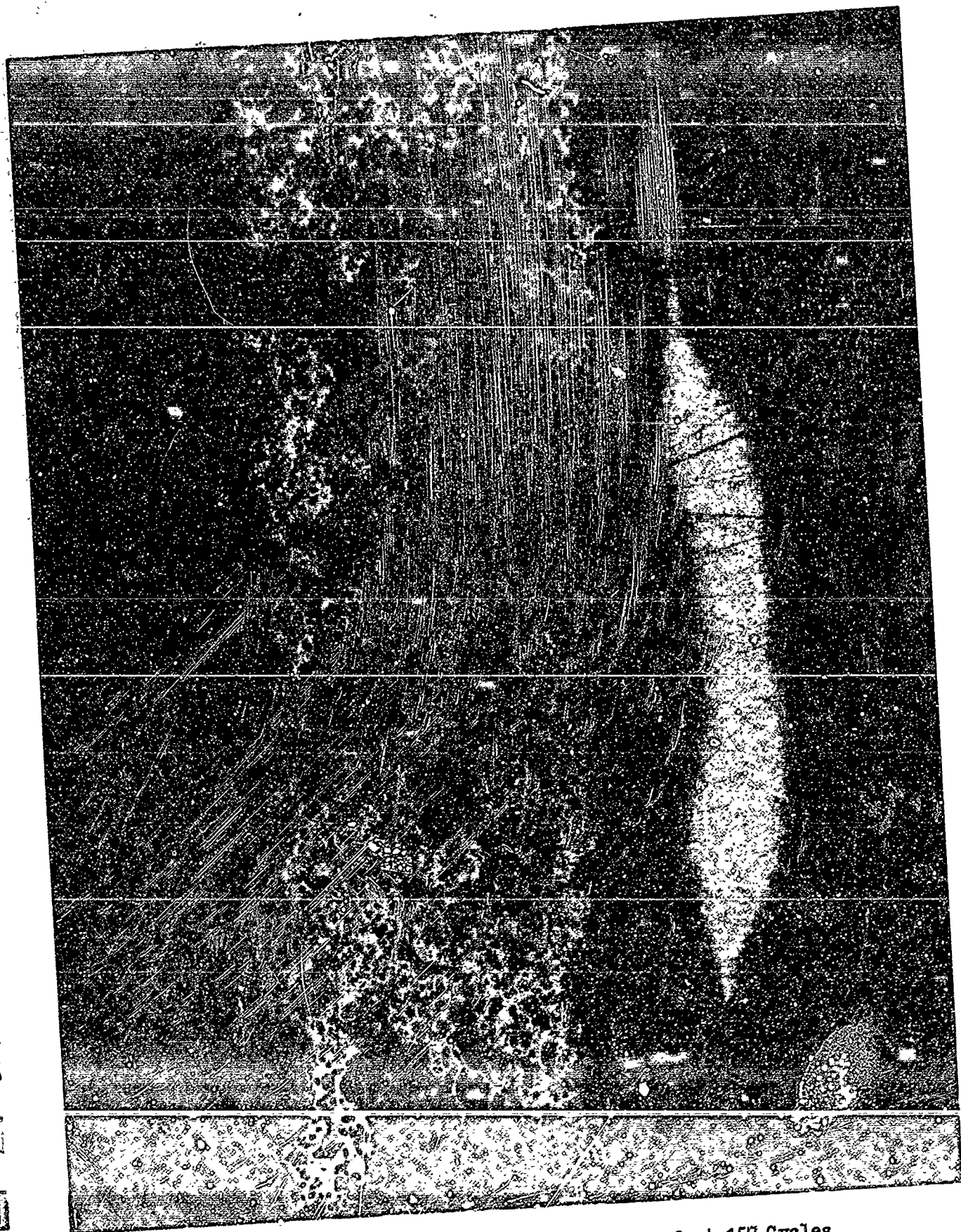


Figure 18. Negative Plate Containing 5% XX-4 ZnO at 157 Cycles

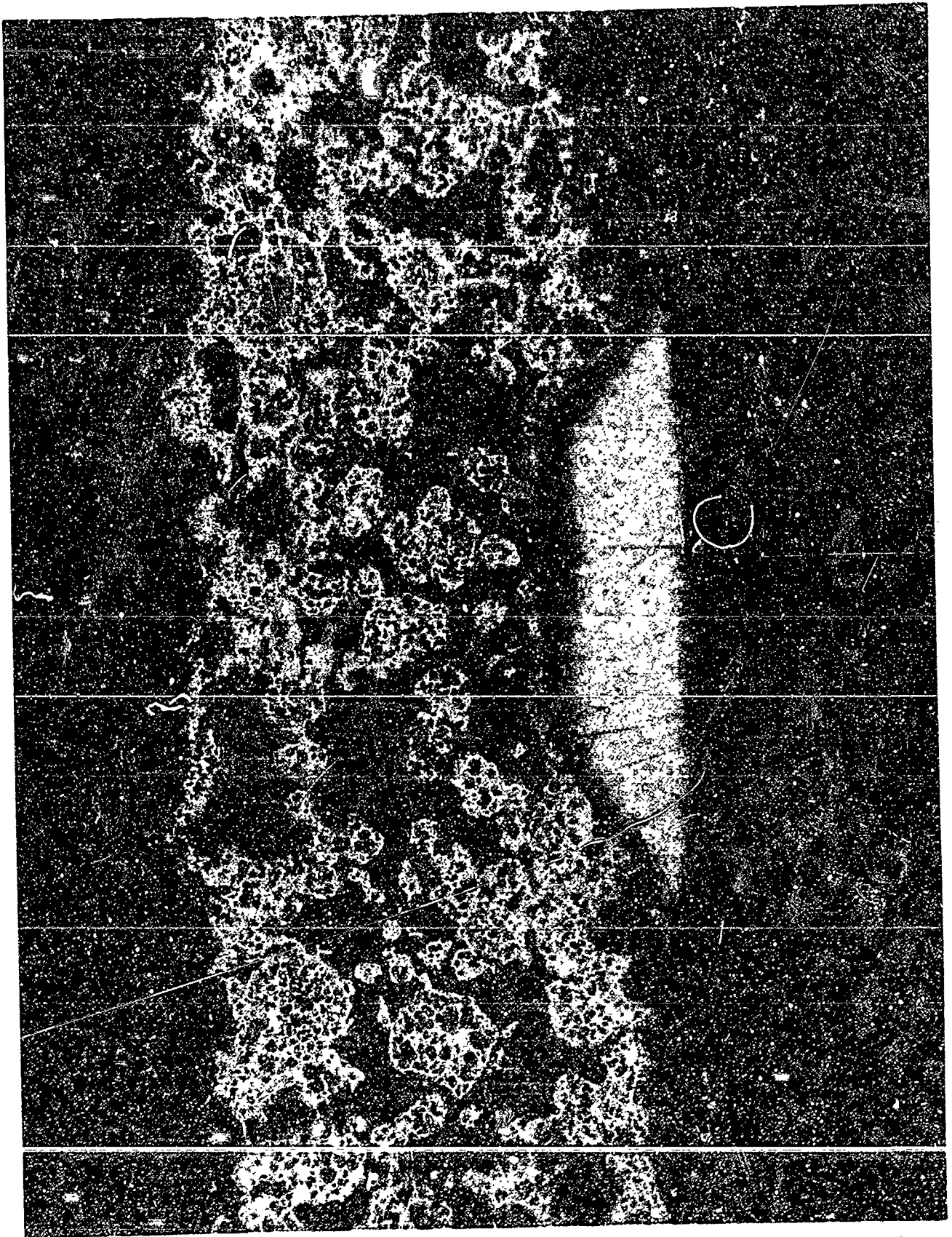


Figure 19. Negative Plate Containing 10% XX-4, ZnO at 157 Cycles

All cells cycled at 60% DOD

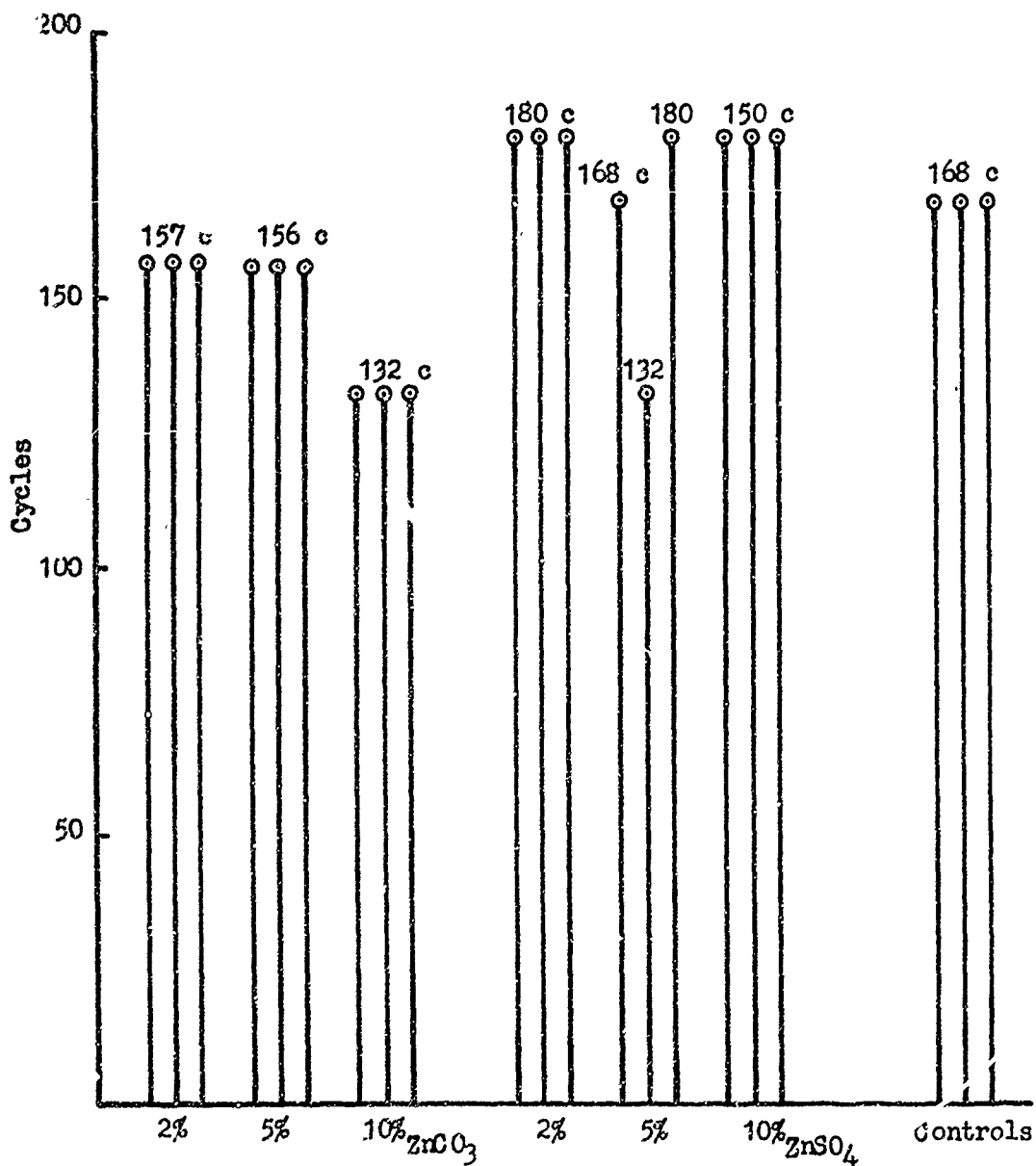


Figure 20. Number of Cycles Obtained by Cells Using ZnCO₃ and ZnSO₄ in the Negative Plate

Cells cycled at 60% DOD

- - - Cycles obtained by control cells in overall program

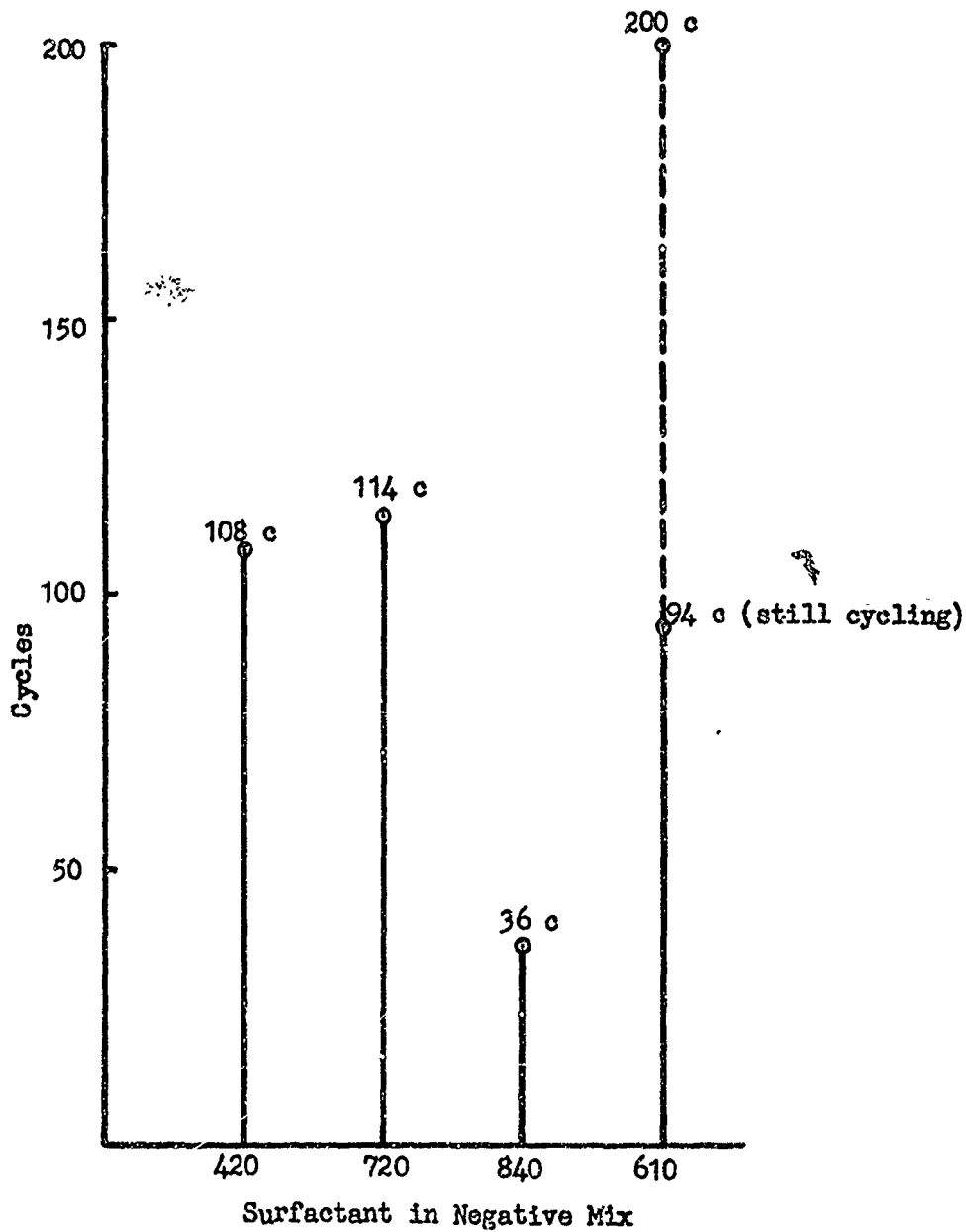


Figure 21. Number of Cycles Obtained by Cells Containing Various Surfactants

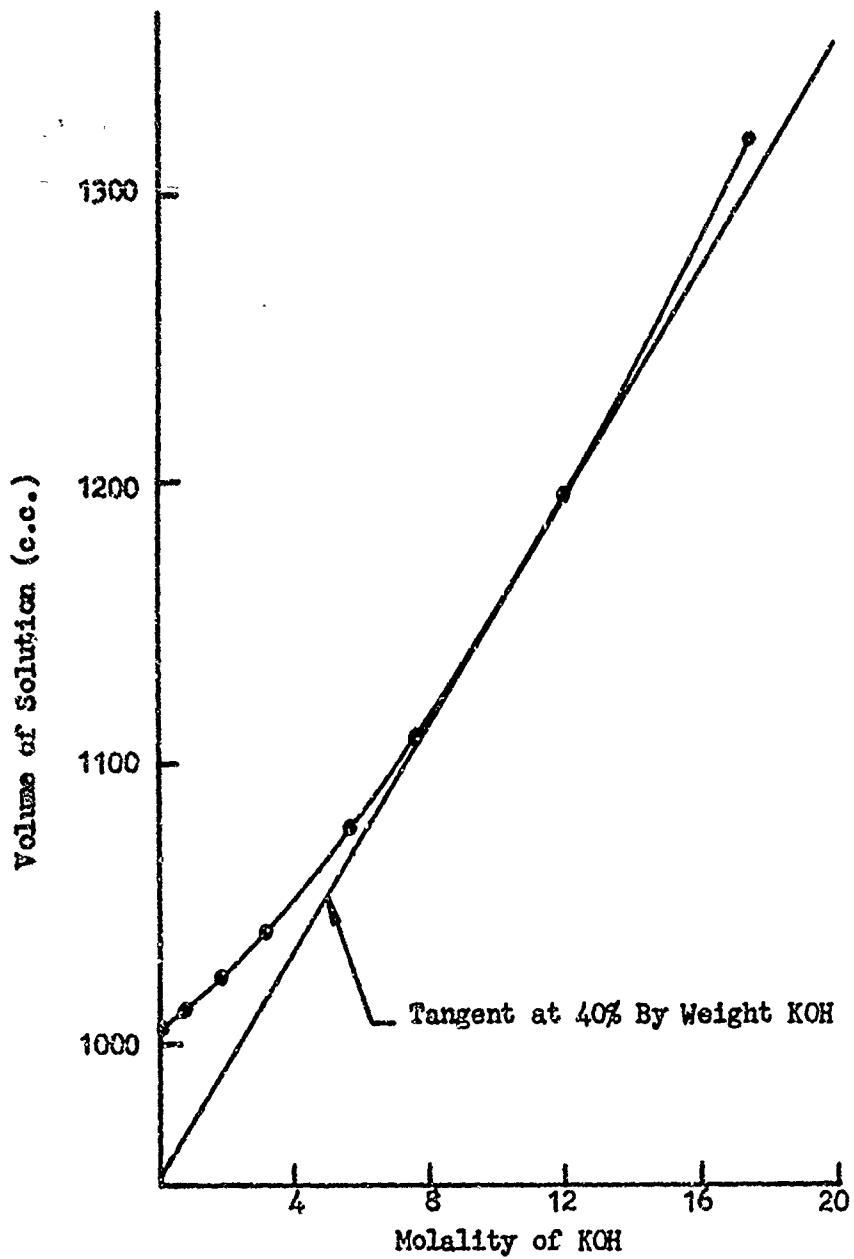


Figure 22. Volume vs. Molality KOH Solutions at 68°F.

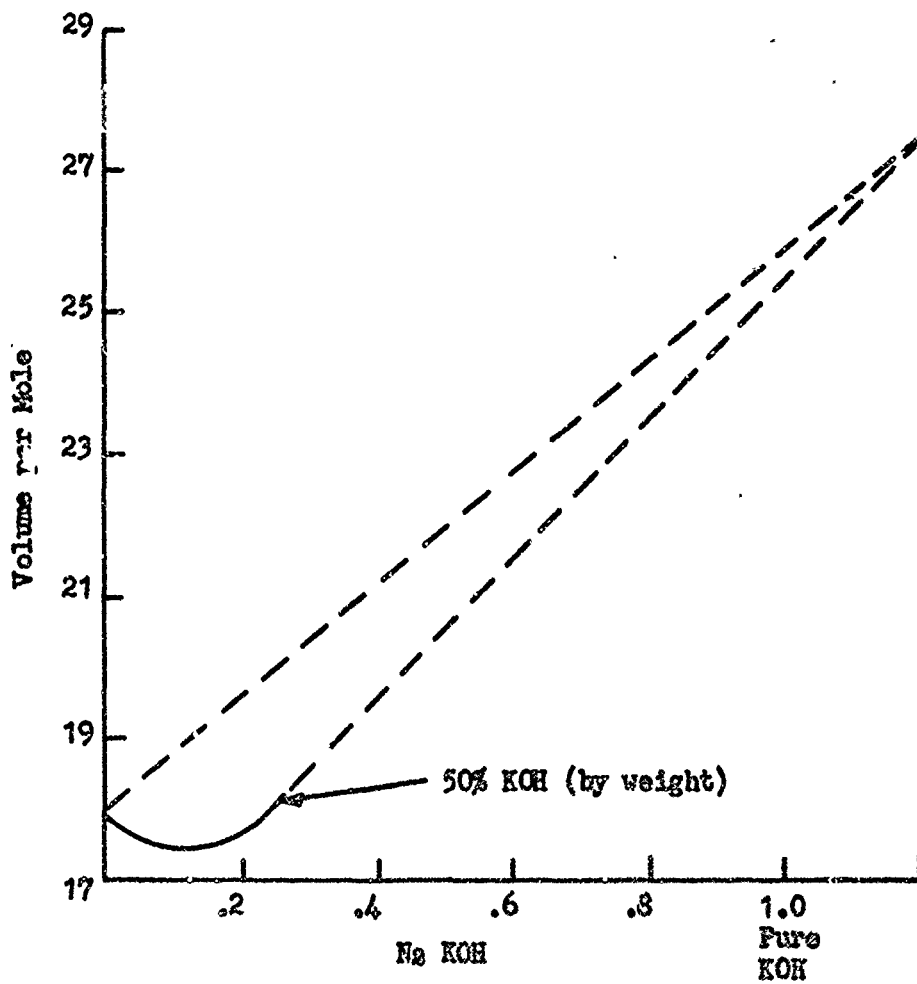


Figure 23. Non-Ideality of KOH Solutions

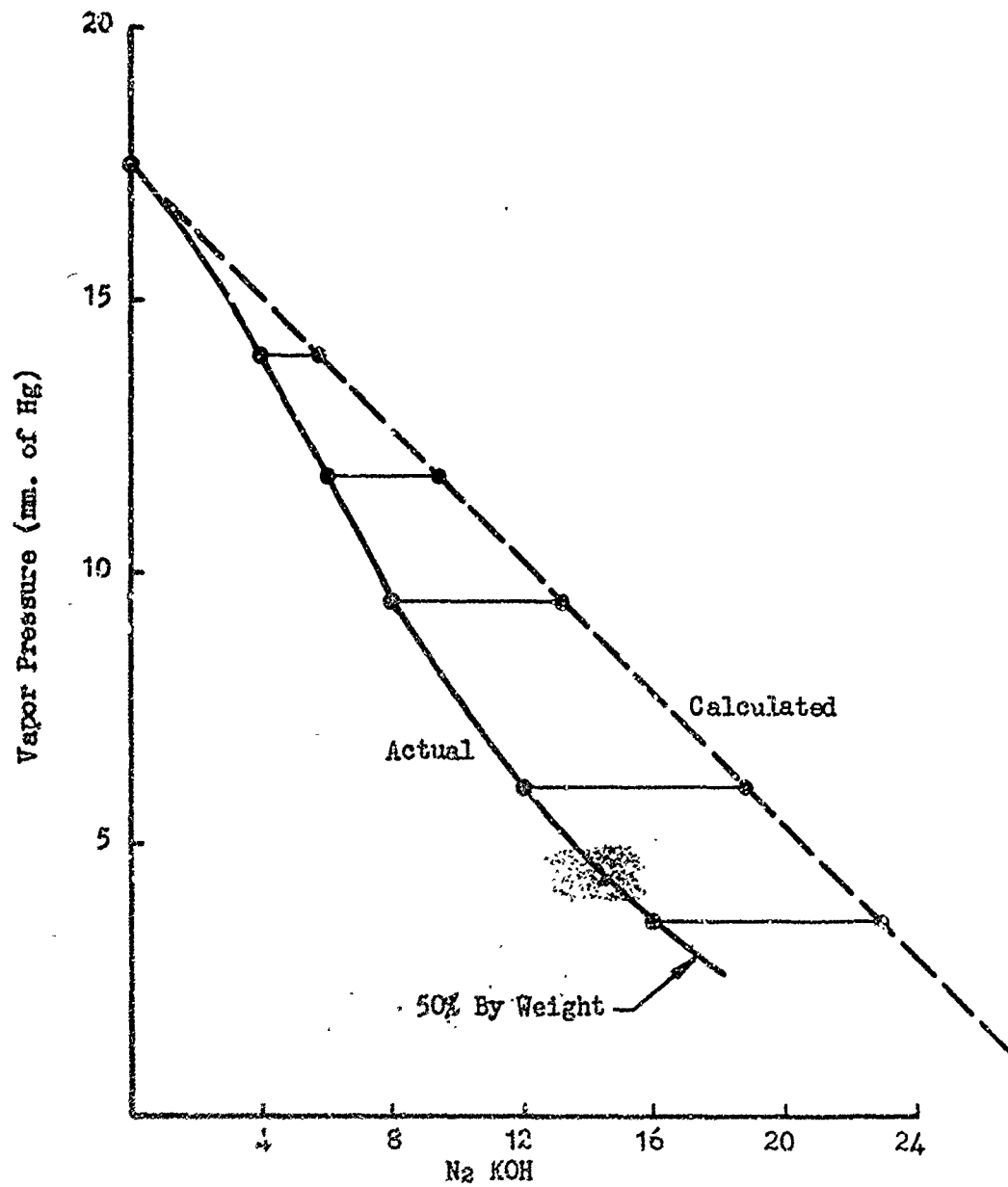


Figure 26. Vapor Pressure of Solutions of KOH, 68°F

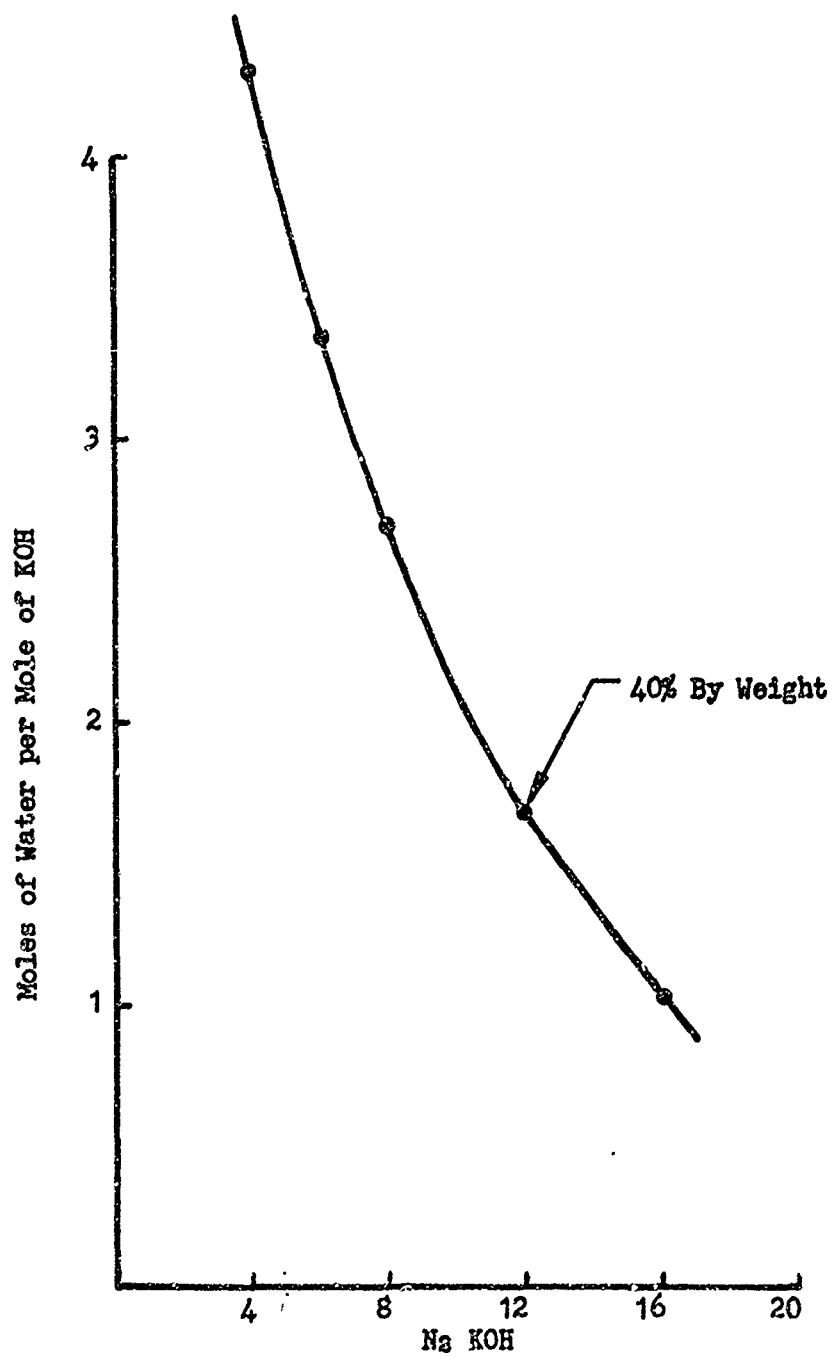


Figure 25. Hydration of KOH, 68^oF.

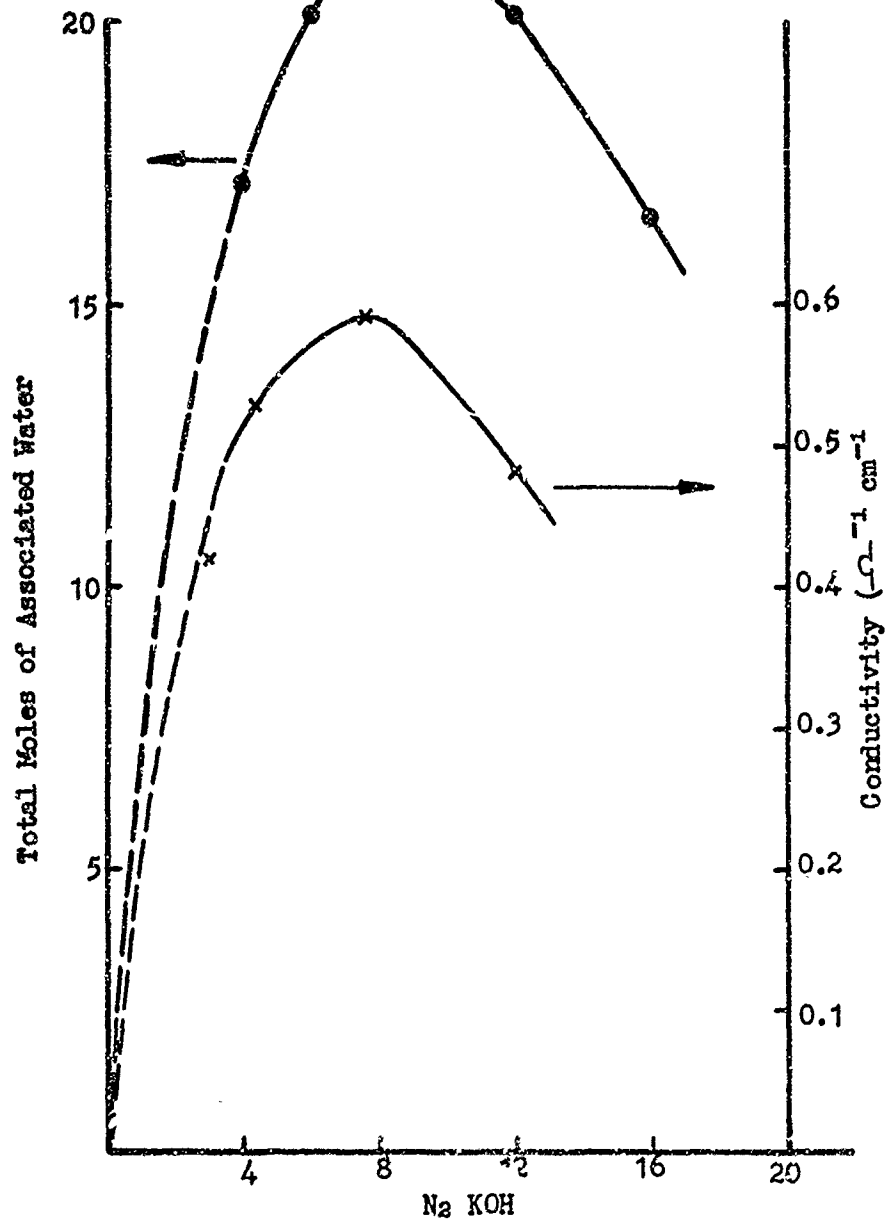


Figure 26. Bound Water vs. KOH Concentration. 68° F

APPENDIX I

FIRST QUARTERLY REPORT

INFLUENCE OF TRANSPORT CHARACTERISTICS
OF SEPARATORS ON CELL ELECTROLYTE DISTRIBUTION

August - November 1966

by

A. H. Remanick, M. Shaw and Wm. I. Nelson

prepared for

Delco-Remy
Division of General Motors
Anderson, Indiana

December 16, 1966

Whittaker
CORPORATION

NARMCO RESEARCH & DEVELOPMENT DIVISION
3540 Aero Court • San Diego, California 92123

ABSTRACT

Diffusion constants of potassium hydroxide through three types of typical separators have been measured at 30° C. The diffusion constants show a marked dependence on concentration although there appears to be no simple relationship between concentration range and diffusion constant.

SUMMARY

A program has been initiated with the purpose of determining membrane parameters governing ionic transport in a silver oxide-zinc cell. During later phases of the program, these parameters will be used to evolve practical mathematical expressions relating cell voltage as a function of time, temperature, current, and concentration, and containing constants specific to the cell construction parameters. Such relationships will be of value in designing cells having improved low temperature performance.

During this period, a method was developed for determining the diffusion constant of KOH through a membrane separating electrolyte solutions of different concentrations. The method is reproducible, involving an average error of 1-5%.

Diffusion constants were determined for PUDO-600 cellophane, Visking V-7 separator, and 2. ZXH 20% acrylic grafted polyethylene over four concentration ranges at 30° C. In addition to the difference in diffusion rate among the membranes at the same concentration range, a marked difference in diffusion rate was exhibited by each membrane over the four concentration ranges investigated. At the present time, there appears to be no simple correlation between the diffusion constant and concentration range.

I. INTRODUCTION

Scaled silver oxide secondary batteries designed for long cycle life have had relatively poor performance at temperatures below ambient and at cycle depths greater than 25%. This is particularly true when the batteries are cycled under a combination of these conditions. Loss in performance further occurs as a function of the rate (current density) at which the battery is discharged at reduced temperatures. At moderately high rates, the performance is improved due to internal heating of the battery. Comparison of cells made with identical plates but with different membrane separator systems leads to the conclusion that major differences in performance can be associated with variations in separator properties. There has been a recent effort to develop new separators which would overcome some of the problems inherent in the existing materials. The use of such materials has still not prevented a decrease in cell performance as a function of discharge rate and low temperature.

Figure 1 shows the effect of temperature on the discharge curve of two cells constructed with membrane separators having different resistivities.

Figure 2 shows the plateau voltage of the cells as a function of temperature. The lower voltage for Cell B is indicative of a higher membrane resistance. The variation of cell impedance with decreasing temperature is comparable for the two cells. In spite of this, Figure 3 illustrates that while little difference in capacity is observed at normal temperatures, this difference increases with decreasing temperature. This suggests that there is some property of the membrane contributing to the decreased capacity of Cell B apart from its higher resistivity.

It is Narmco's belief that this differential loss in capacity with decreasing temperature is associated with changes in electrolyte distribution brought

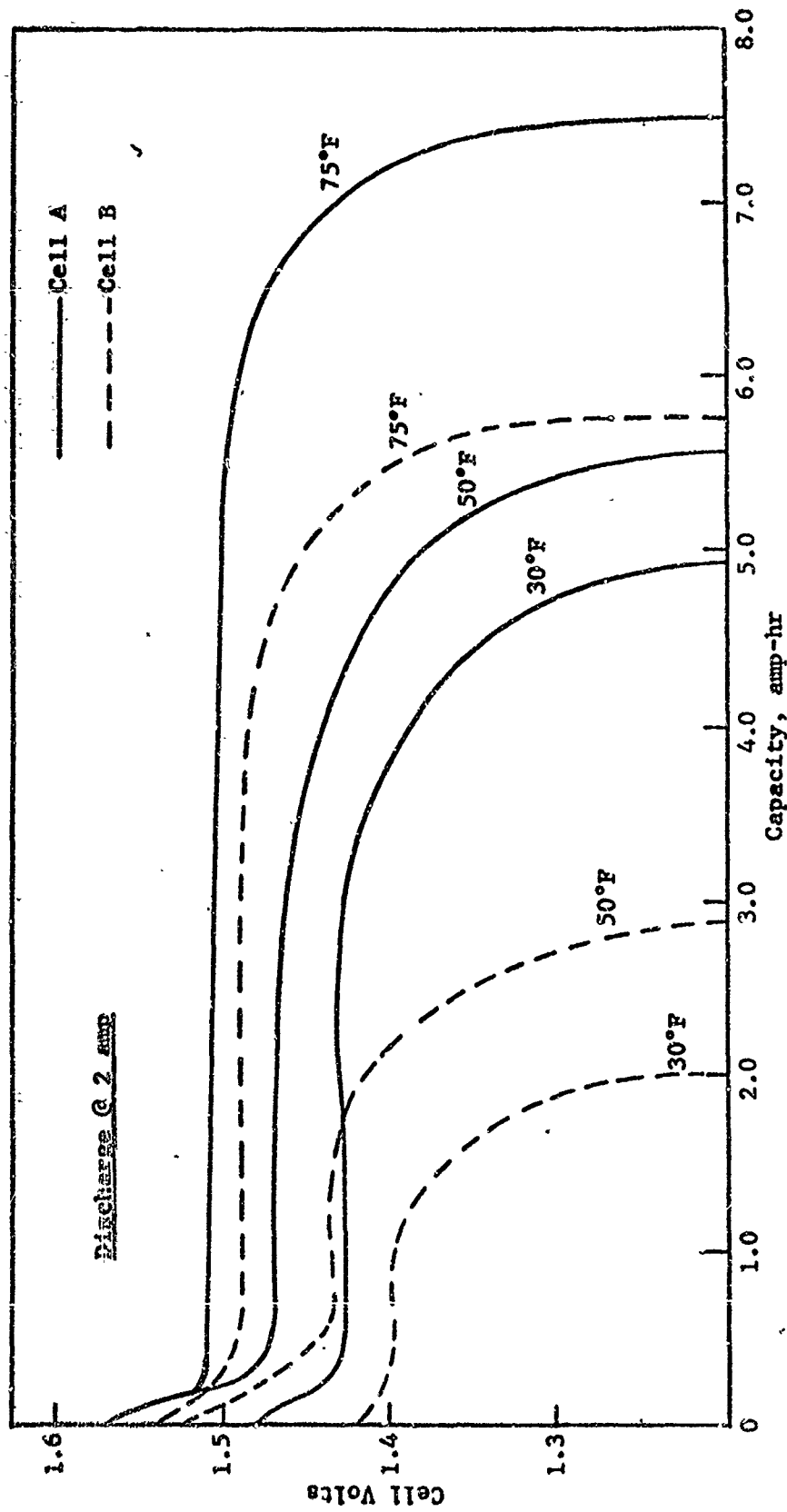


Figure 1. Effect of Temperature on Discharge of Cells with Different Membranes

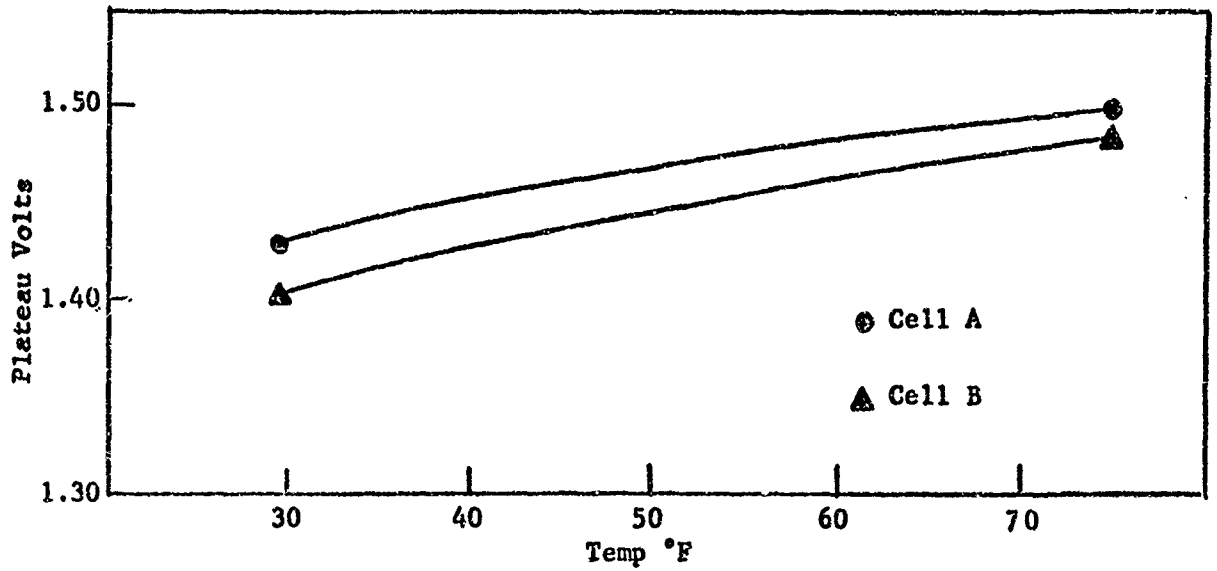


Figure 2. Effect of Temperature on Plateau Voltage

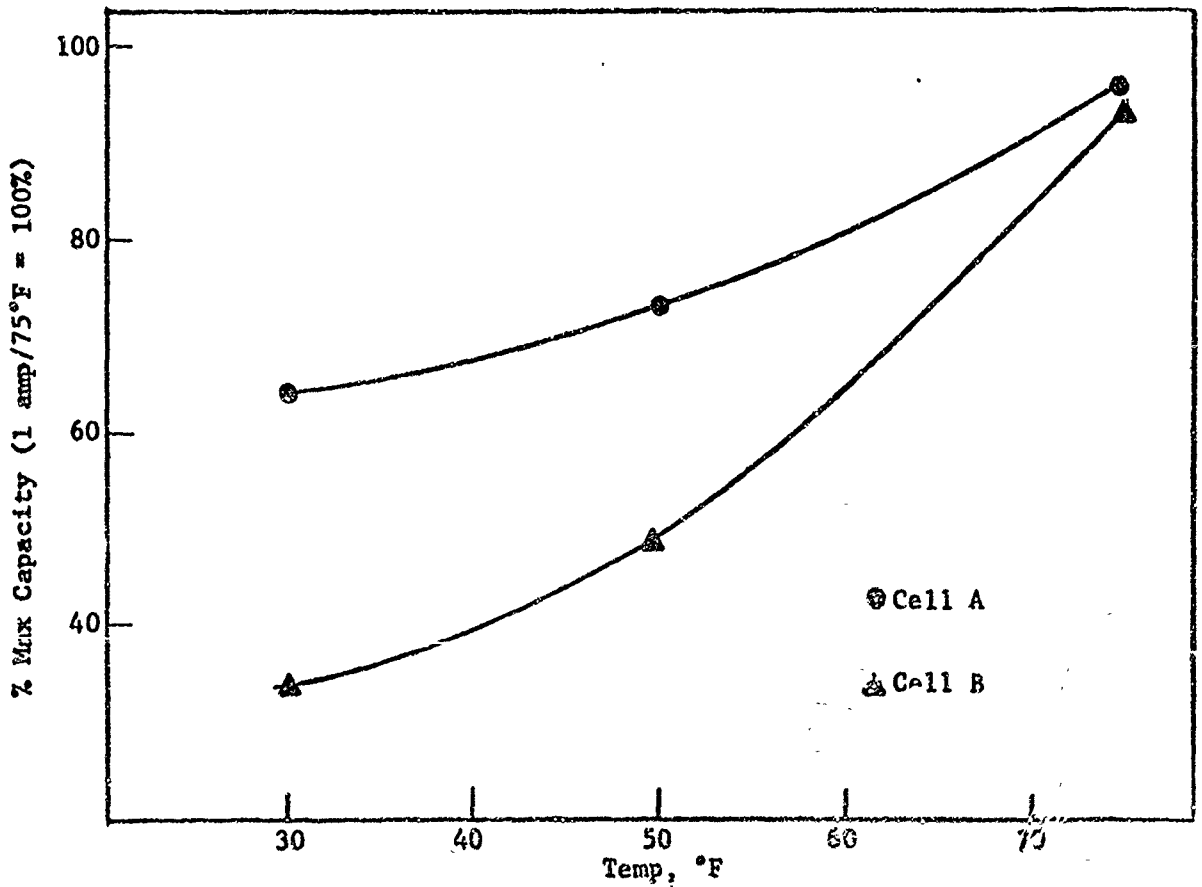
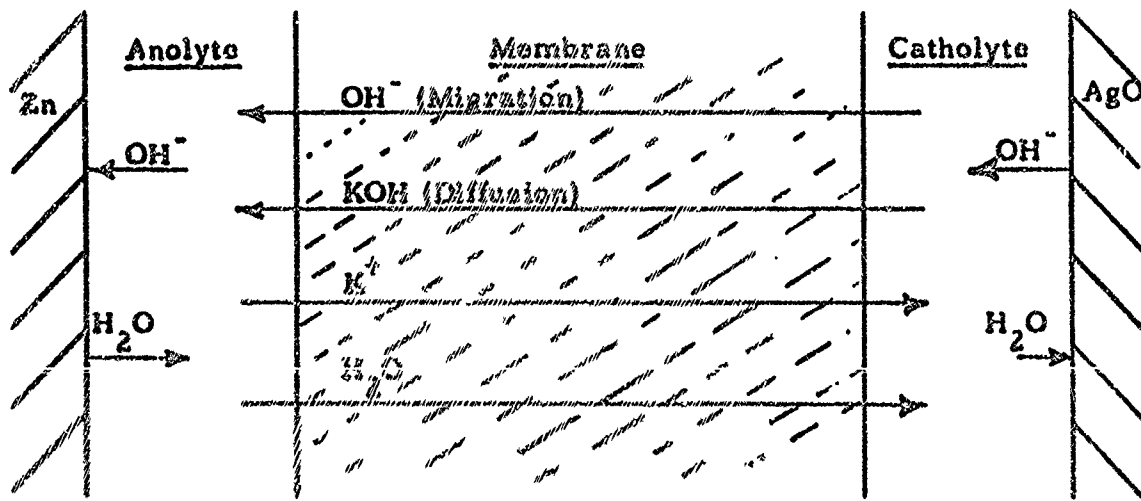


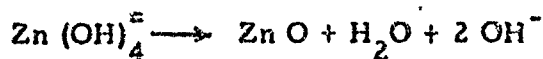
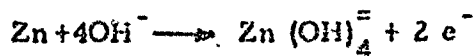
Figure 3. Effect of Temperature on Capacity

about by the restricted movement of ions through the membrane, the degree of this restriction being a function of the membrane properties, as well as of the cell construction parameters. The purpose of this program is to define and evaluate those membrane parameters which influence ionic movement in the cell, and to mathematically correlate these parameters and the cell construction parameters, with changes in electrolyte concentration, in order to predict cell operating characteristics under varying conditions. The program goal is to evolve practical mathematical expressions relating cell voltage as a function of time, temperature, current, and concentration, and containing constants specific to the cell construction parameters including the transport characteristics of the membrane separators. Such relationships will be of value in the design of cells having low-temperature performance.

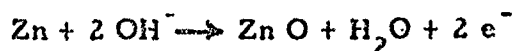
The following schematic is a representation of the silver oxide-zinc system showing the anolyte and catholyte compartments and the membrane separator, including the directions of movement of ions and water under conditions of discharge.



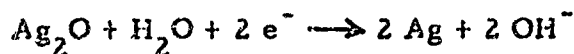
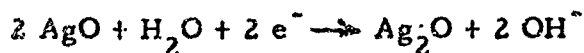
The anode-anolyte process involves the following reactions:



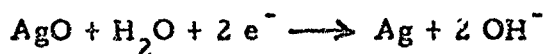
resulting in the net reaction



The cathode-catholyte process involves the following reactions:



resulting in the net reaction



In order to indicate the types of measurements which will be obtained in the program, a brief analysis of the ionic transport processes occurring on discharge is given below. Since these expressions are only presented in order to indicate the types of measurements involved in the program, some simplifying assumptions were used to obtain these equations.

The rate of removal of hydroxyl from the anolyte as a result of the zinc discharge reaction is proportional to the current, i. e.

$$\text{rate of OH}^- \text{ depletion} = -k_1 i \quad (1)$$

Hydroxyl ion is being produced at the cathode simultaneously however, and will reach the anolyte at a rate determined by the migration component of the current, i. e.

$$\text{rate of OH}^- \text{ replenishment} = k_2 i t \quad (2)$$

where t^- is the transference number of OH^- in the separator, and k_1 contains the Faraday constant and time factor. Since t^- is necessarily less than unity, the concentration of hydroxide in the anolyte must increase resulting in increasing depletion of hydroxyl ion. The concentration gradient thereby created introduces a second mechanism by which OH^- is restored, namely diffusion, i. e.

$$\text{rate of } \text{OH}^- \text{ replenishment} = k_2 \left(\frac{\text{OH}_c^-}{V_c} - \frac{\text{OH}_a^-}{V_a} \right) \quad (3)$$

where the bracketed term represents the concentration difference, and k_2 includes the diffusion constant of hydroxyl ion* in the separator and the membrane thickness. OH_c^- and OH_a^- are the total amounts of hydroxyl ion in the catholyte and anolyte respectively. V_c and V_a are the corresponding volumes.

Similar expressions may be derived for the rate of change of OH^- in the catholyte.

It should be noted that the expressions for the changes in anolyte and catholyte concentrations are applicable for both charge and discharge conditions, bearing in mind the correct meaning of the terms anolyte and catholyte. To avoid misinterpretation, these are defined as follows:

Anolyte - that portion of the electrolyte adjacent to that electrode where an oxidation process occurs, namely, at the anode. On discharge this is the negative plate (e.g. Zn), but on charge it is the positive plate (e. g. Ag).

Catholyte - that portion of the electrolyte adjacent to that electrode where a reduction process occurs, namely, at the cathode. On discharge this is the positive plate (e. g. AgO), but on charge it is the negative plate (e. g. ZnO).

*The term "diffusion constant of hydroxyl ion" is used for mathematical simplicity since it is well known that diffusion coefficients of molecular species must involve both anion and cation.

Inspection of equations 1, 2 and 3 indicates that in order to determine concentration changes within the various portions of the cell, it will be necessary to determine:

1. The diffusion constant of KOH in the separator as a function of concentration and temperature.
2. The transference numbers of K^+ , OH^- , and water within the separator as a function of concentration and temperature.
3. The amount of KOH in the membranes as a function of concentration and temperature.

With the above information and specific constants relevant to cell construction, it will then be possible to derive more accurate relationships concerning concentration change with time.

Diffusion of Electrolyte

The first phase of the program is concerned with the measurement of KOH diffusion through typical separator materials. The diffusion measurements are made by use of a typical diaphragm cell (Ref. 1) wherein the usual sintered glass diaphragm is replaced with the membrane to be studied. This type of cell consists of two chambers separated by a membrane having an area A exposed to each of the chambers. Each chamber is filled with a known volume of solution of specified concentration.

Using Fick's first law

$$J = D \frac{\partial c}{\partial x} \quad (4)$$

the amount of material into one chamber under steady state conditions is given as

$$\frac{1}{A} \frac{d(c'V')}{dt} = D \frac{(c''-c')}{\Delta x} \quad (5)$$

where c' , V' are the concentration and volume respectively, of the particular chamber under consideration, D is the diffusion coefficient, and Δx is the membrane thickness. Good mixing of the chamber contents is maintained such that the only possible concentration gradient ($c''-c'$) appears across the membrane.

If conditions are chosen such that V' remains constant, equation 5 may be rearranged to give

$$\frac{dc'}{dt} = \frac{AD'}{V'} (c''-c') \quad (6)$$

where

$$D' = \frac{D}{\Delta x}$$

Under steady state conditions, the amount of material passing into one chamber must be equal to the amount of material passing out of the other chamber. Therefore an expression similar to equation 6 is given as

$$\frac{dc''}{dt} = -\frac{AD'}{V''} (c''-c') \quad (7)$$

Combination of equations 6 and 7 gives

$$\frac{dc''}{dt} - \frac{dc'}{dt} = -AD' (c''-c') \left[\frac{1}{V'} + \frac{1}{V''} \right] \quad (8)$$

which may be rearranged to give

$$\frac{d(c''-c')}{(c''-c')} = -AD' \left(\frac{1}{V'} + \frac{1}{V''} \right) dt \quad (9)$$

Integration of equation 9 yields

$$\ln \frac{(c''-c')_t}{(c''-c')_0} = -AD' \left(\frac{1}{V'} + \frac{1}{V''} \right) t \quad (10)$$

Therefore, D' may be evaluated by measuring the concentration in both chambers at specific time intervals provided that conditions are chosen so

that the volume term in equation 10, $\left(\frac{1}{V'} + \frac{1}{V''}\right)$ remains essentially constant.

An alternate experimental approach is indicated by equation 6. If the chamber containing solute at concentration c'' is made very large with respect to the other chamber, c'' will be essentially constant. Under these conditions, rearrangement and integration of equation 6 gives

$$\ln \frac{c''_0 - c'_t}{c''_0 - c'_0} = \frac{-AD'}{V} t \quad (11)$$

Under experimental conditions based on equation 10, D' is evaluated from a plot of $\ln (c'' - c'_t)$ vs t . Similarly, for equation 11, D' is evaluated using the term $\ln (c''_0 - c'_t)$. Therefore, it is not necessary to determine t_0 accurately, since any value of t may be used as t_0 . Thus, sufficient time may be allowed before measurement in order for the membrane to approach steady state condition. Furthermore, any set of initial concentrations may be used to determine D' , thereby allowing measurement of the effect of concentration range on D' .

The latter criteria is probably the main objection to the method detailed by Harris (Ref. 2). In this method, use of equation 6 is made by properly adjusting experimental conditions. Thus, if $c'' - c'$ is kept essentially constant during the measuring period, then equation 6 reduces to the zero order expression

$$\frac{dc'}{dt} = k \quad (12)$$

where $k = \frac{AD'}{V} (c'' - c')$

Integration of equation 11 yields

$$c' = k t \quad (13)$$

Experimentally, the method described by Harris uses water in one chamber and KOH of relatively high concentration in the other. Under these conditions, if the amount of change of c' is small, then $c'' - c' \approx c''$. The value of c' is determined by pH measurement. Although the technique is relatively rapid and convenient, it suffers from the fact that a concentration far different from that actually occurring in an electrochemical cell is seen by one side of the membrane. Although it appears that D' as measured by this method (Ref. 3) is insensitive to the concentration on the "high" side of the membrane, an alternate method of measurement (as previously described) is necessary for complete characterization.

II. RESULTS

Initial measurements of KOH diffusion constants through membranes were made on the basis of equation 10. The values of c'' and c' were followed by removal of small samples at fixed time intervals and titration with dilute acid. However, it was found that this method did not afford reproducible results. The non-reproducibility was traced to the sampling techniques involved in the method.

In order to improve the accuracy of the method, an alternate experimental procedure, based on equation 11, was adopted. This involved continuous monitoring of density in the smaller chamber of a two-compartment cell (Figure 4). Density measurements were made by determining the weight of a sinker immersed in the liquid under study (Figure 5). Determination of the sinker weight in air and in distilled water would then allow calculation of the molarity of the solution since density-molarity relationships had been previously established (Ref. 4).

In practice, it was found that the actual calculation was not necessary. From the data of Akerlof and Bender (Ref. 4), it can be shown that

$$c = kd + a \quad (14)$$

where c and d are the concentration and density respectively of the KOH solution, and k and a are arbitrary constants. Combining equations 11 and 14 yields

$$\ln \frac{d''_o - d'_t}{d''_o - d'_o} = \frac{-AD'}{V} t \quad (15)$$

Using the buoyancy method the density may be expressed as

$$d = \frac{w_a - w_l}{V} \quad (16)$$

where w_a and w_l are the weights of the sinker in air and liquid respectively, and V is the sinker volume. Combining equations 15 and 16 yields

$$\ln \frac{w_o'' - w_t'}{w_o'' - w_o'} = \frac{-AD'}{V} t \quad (17)$$

Therefore, D' can be calculated directly from w_o'' and w_t' . In practice, the compartment corresponding to w' contained the higher concentration and smaller volume. The expanded form of equation 17

$$\log (w_o'' - w_t') - \log (w_o'' - w_o') = 2.303 \frac{AD'}{V} t \quad (18)$$

was used for the actual calculation* of D' .

Three types of membranes, PUDO-600 cellophane, Visking V-7 separator, and 2,2XH 20% acrylic acid graft polyethylene, were studied during this period. Four concentration ranges were investigated. The values of D' for each type of membrane is given in Table I.

For convenience, the results have been expressed in the units of $\text{ml min}^{-1} \text{in}^{-2}$. The flux per unit area across one layer of membrane may be quite readily calculated by multiplying the value of D' by the proper concentration gradient in units of moles ml^{-1} . It can be readily seen that the units of D' are equivalent to the usual units of the diffusion coefficient, $\text{cm}^2 \text{sec}^{-1}$.

*Initially, calculation of D' was made by the least squares method using a desk calculator. More recently, a program has been written for an Olivetti-Underwood Programma 101 digital computer in order to facilitate calculation of both D' and its average error.

TABLE I
KOH DIFFUSION CONSTANTS* C^o MEMBRANES 30° C

<u>Membrane</u>	<u>Concentration Gradient</u>			
	<u>2-4, 5M</u>	<u>6-8, 5M</u>	<u>7, 6-10, 1M</u>	<u>9, 5-11, 7M</u>
PUDO-600	0, 196±0, 003	0, 204±0, 003 0, 213±0, 003(a)	0, 191±0, 005	0, 111±0, 002
Visking	0, 127±0, 003	0, 156±0, 002	0, 111±0, 001	0, 0907±0, 0017
2, 2XH	0, 136±0, 004	0, 131±0, 001	0, 148±0, 004 0, 152±0, 005(a)	0, 0936±0, 0038

* ml min⁻¹ in⁻²

(a) second determination using separate sample

III. DISCUSSION

As is readily seen from Table I, the method employed to determine D' gave results which were usually within a precision of 5%, and in most cases even better. The fact that D' determined from duplicate runs of PUDO-600 in the range 6.0-8.5M are slightly outside of the experimental error range would appear to indicate that the uniformity of the membranes themselves are not better than about 5%.

The concentration gradient ranges were chosen in order to determine the effect of concentration on D' . Ideally, one would measure the self-diffusion of KOH by an isotope method. However, since a usable isotope of potassium is unavailable, the present method must be used. Although the membrane is exposed to a different concentration of KOH on each side, it can readily be shown that within the compartment in which the concentration change occurs, the amount of change during the time of measurement is less than 10%. Therefore, the membrane is exposed to reasonably steady state conditions during the measurement. Furthermore, as was previously discussed, it is not necessary to choose any particular zero time, thereby allowing the physical state (temperature, swelling, etc.) within the membrane to reach equilibrium. Irreversible chemical reaction, of course, could have a time dependent effect on the membrane.

We have chosen to use D' as the fundamental quantity determined in this part of the study for the following reason. As previously defined,

$$D' = \frac{D}{\Delta x} \quad (19)$$

where D is the diffusion coefficient of the membrane and Δx is the thickness.

The diffusion constant of the membrane may be equated with the diffusion coefficient of KOH by

$$D = D_{\text{KOH}} \cdot P \quad (20)$$

where P is the permeability of the membrane under the conditions used. Therefore D' may be defined as

$$D' = \frac{D_{\text{KOH}} \cdot P}{\Delta x} \quad (21)$$

From equation 21, it is evident that changes in any or all of three parameters with respect to concentration would affect D' . To attempt to correlate changes in D' with respect to all three parameters in equation 21 would be outside the scope of the present program.

Figure 6 shows a plot of diffusion constant D' against the mean concentration (calculated for each concentration range measured) of KOH in the three membrane types. PUDO-600 exhibits the highest diffusion constant at concentrations 3 to 9 molar. All three membrane types exhibit comparable and low diffusion constants at the highest mean concentration measured (10.6M). PUDO-600 and Visking both exhibit a maximum diffusion constant at 7.75M. The 2.2XH membrane, an irradiated material, differs from the other membranes in that the diffusion constant is fairly constant from 3 to 8M, and then reaches a maximum at a higher concentration range (8.85M compared with 7.75M for PUDO-600 and Visking).

No physical interpretation of the data plotted in Figure 6 will be offered at this time, the primary reason being the choice of a mean concentration of KOH in the membrane. Preliminary measurements have indicated an even higher concentration in the membrane than existing in the original solution. The diffusion constant-concentration data will therefore be more meaningful when data on KOH absorption by the membranes are available later in this program.

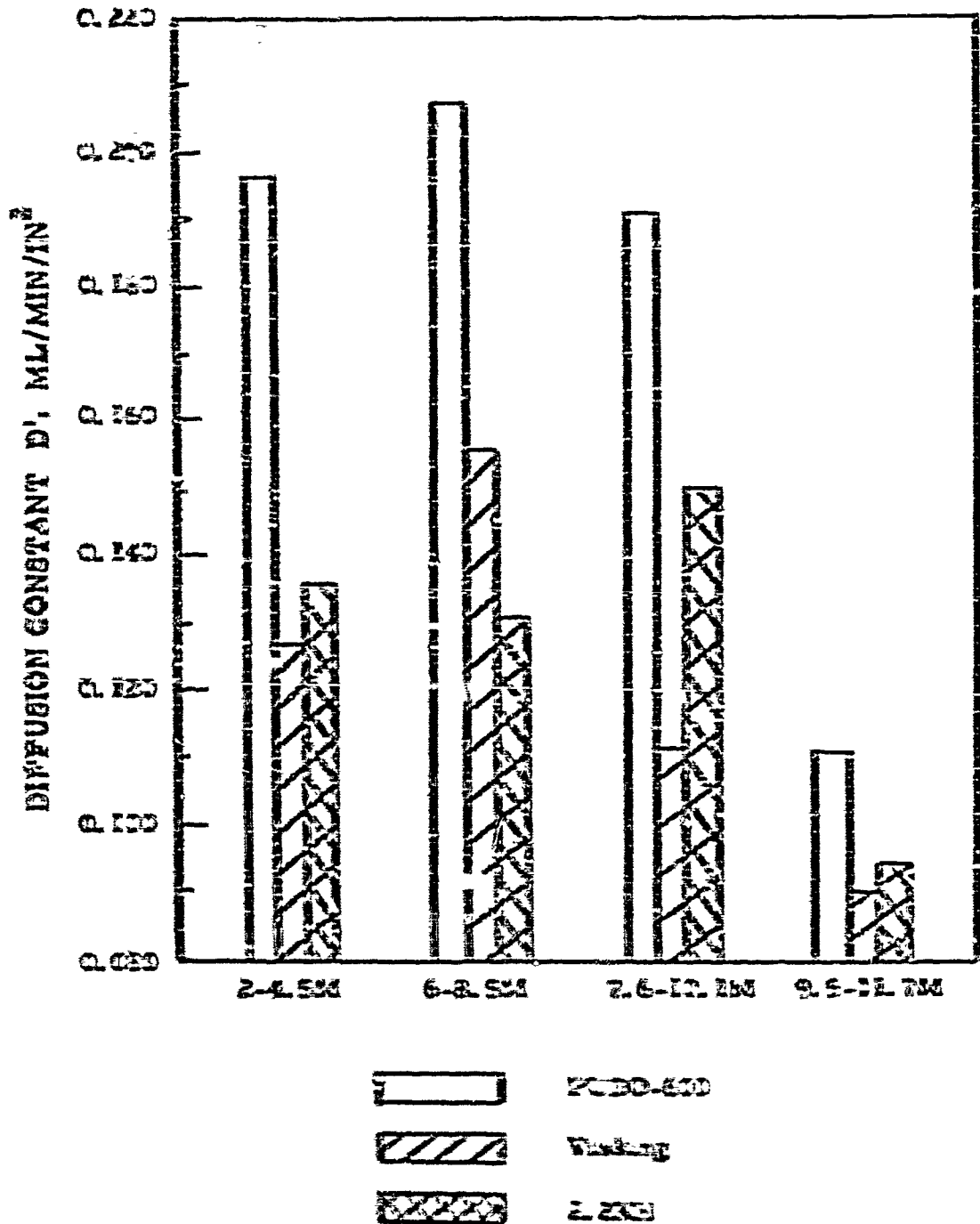


FIGURE 6 - Effect of Concentration Range on Diffusion Constant of Membrane

IV. EXPERIMENTAL

1. Determination of Diffusion Rates

The cell (Figure 4) was assembled after placing a small segment of the test membrane in the membrane holder. The purpose of the membrane holder was to vary the orifice size between the two chambers. The maximum size orifice was obtained by removing the membrane holder and placing the membrane directly between the face plates of each chamber.

After assembly, the small compartment of the cell was filled with 100.0 ml KOH of the higher concentration to be used for the particular run. The larger compartment was filled to the same liquid level with KOH of the lower concentration. The volume of solution was usually 1300 ml in the larger compartment. Magnetic stirring bars were placed in each compartment.

The cell was then placed in the constant temperature bath (Figure 5). A Plexiglass sinker, weighted with lead to adjust apparent density, was suspended by means of a platinum wire from a hook extended below the balance. A Mettler B5 analytical balance had been modified by means of a Mettler GD adapter, for determining weights of material suspended below the balance. The cell was positioned and then raised so that the top of the sinker was about one inch below the liquid level in the large compartment. Stirring of both solutions was then started.

After about two hours equilibration, readings of the sinker weight were determined. (The stirrer was stopped during the readings, and the solution was allowed to come to rest for about 30 seconds.) Readings were continued at 15-20 minute intervals until a consistency of about 0.3 mg was

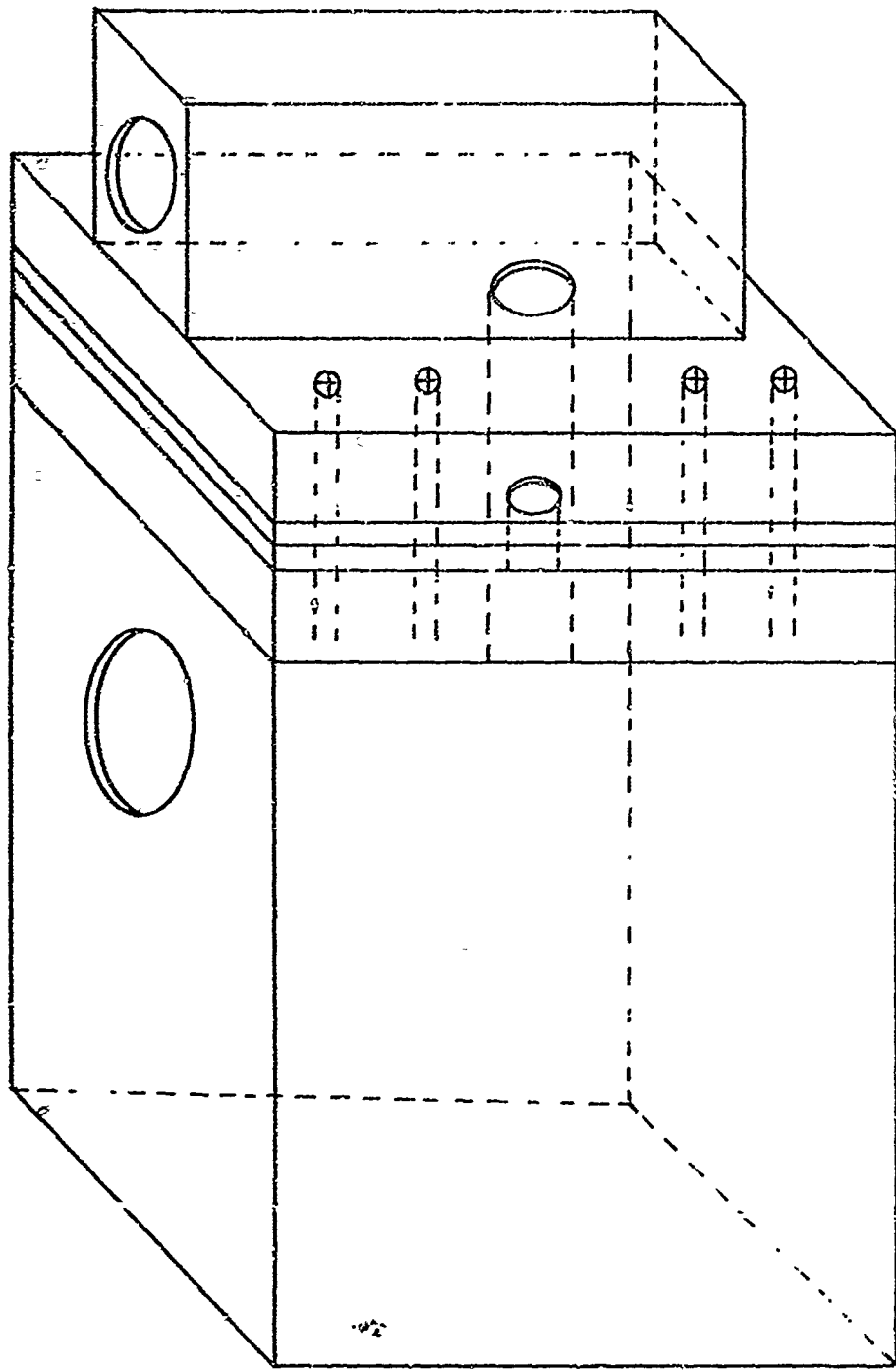
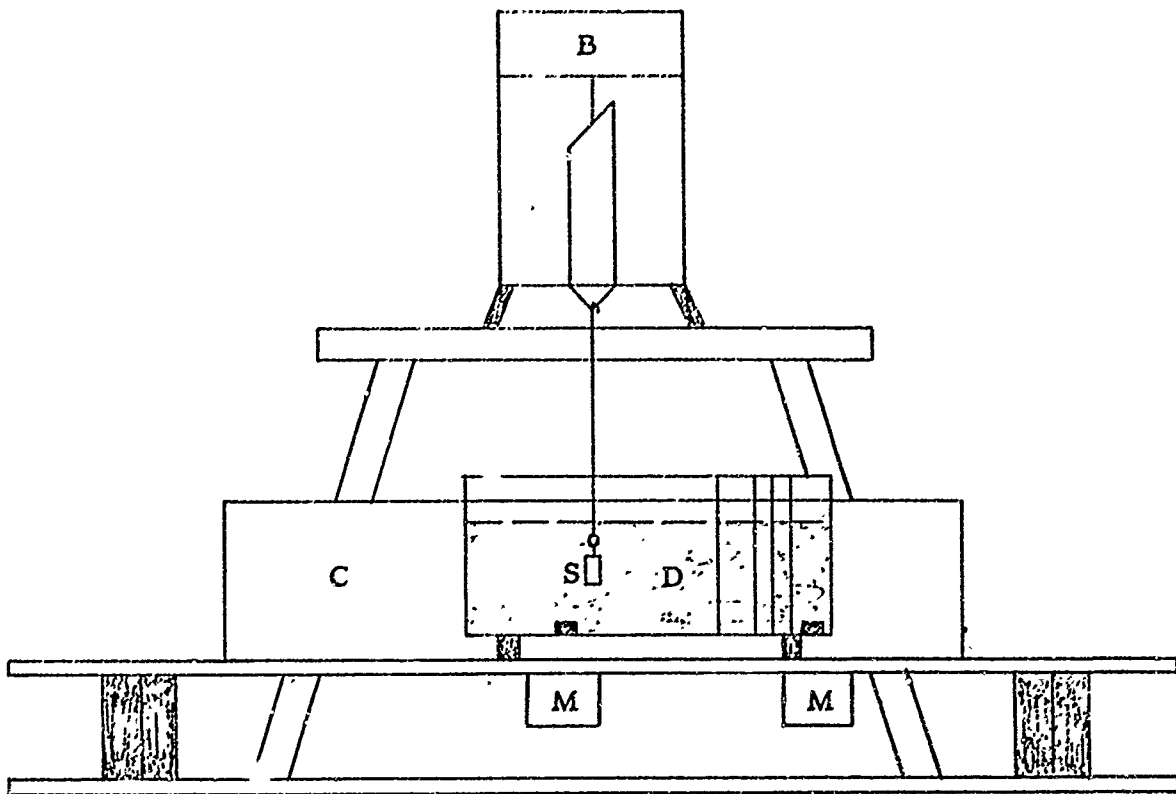


FIGURE 4 - Diffusion Cell



- B - Balance
- C - Constant temperature bath
- D - Diffusion cell
- M - Magnetic stirrers
- S - Sinker

FIGURE 5 - Diffusion Measurement Apparatus

reached. The sinker was then transferred to the smaller compartment. After an equilibration period of 30 minutes, measurements of the sinker weight at fixed time intervals were made. Usually 13 points were then taken over a three-hour period. Typical data are given in Table II, and are presented graphically in Figure 7.

The fact that the KOH concentration in the large compartments remains invariant can readily be seen by the following relationships:

$$\begin{aligned}\text{Maximum Total Flux} &= D' \times \text{Area} \times \text{total time} \times \text{maximum gradient} \\ &= 0.2 \text{ ml min}^{-1} \text{ in}^{-2} \times 0.5 \text{ in}^2 \times 180 \text{ min} \times 2.5 \times 10^{-3} \text{ moles ml}^{-1} \\ &= \underline{0.045 \text{ moles}}\end{aligned}$$

The total amount of KOH in the large compartment is 1.3 liters \times 6.0 moles/liter or 7.2 moles. Therefore, the percent of change in the large compartment is $\frac{0.045}{7.2} \times 100$ or 0.6%.

A similar analysis indicates that the change in concentration in the smaller compartment is of the order of 5%.

TABLE II

EXPERIMENTAL DATA FOR DIFFUSION OF KOH WITHIN PUDO - 600

Run No. 15E

Orifice area ----- 0.500 in²

Large Compartment -- 6.0M

Small Compartment -- 8.5M

Temperature ----- 29.9°C

<u>Large Compartment</u>		<u>Small Compartment</u>	
<u>Elapsed Time</u> <u>Minutes</u>	<u>Sinker Weight</u> <u>gms</u>	<u>Elapsed Time</u> <u>Minutes</u>	<u>Sinker Weight</u> <u>gms</u>
0	2.7546	0	2.4371
15	2.7530	18	2.4417
30	2.7528	30	2.4457
45	2.7528	45	2.4501
60	2.7526	60	2.4550
		75	2.4599
		90	2.4647
		105	2.4688
		120	2.4730
		135	2.4777
		150	2.4825
		165	2.4864
		180	2.4904

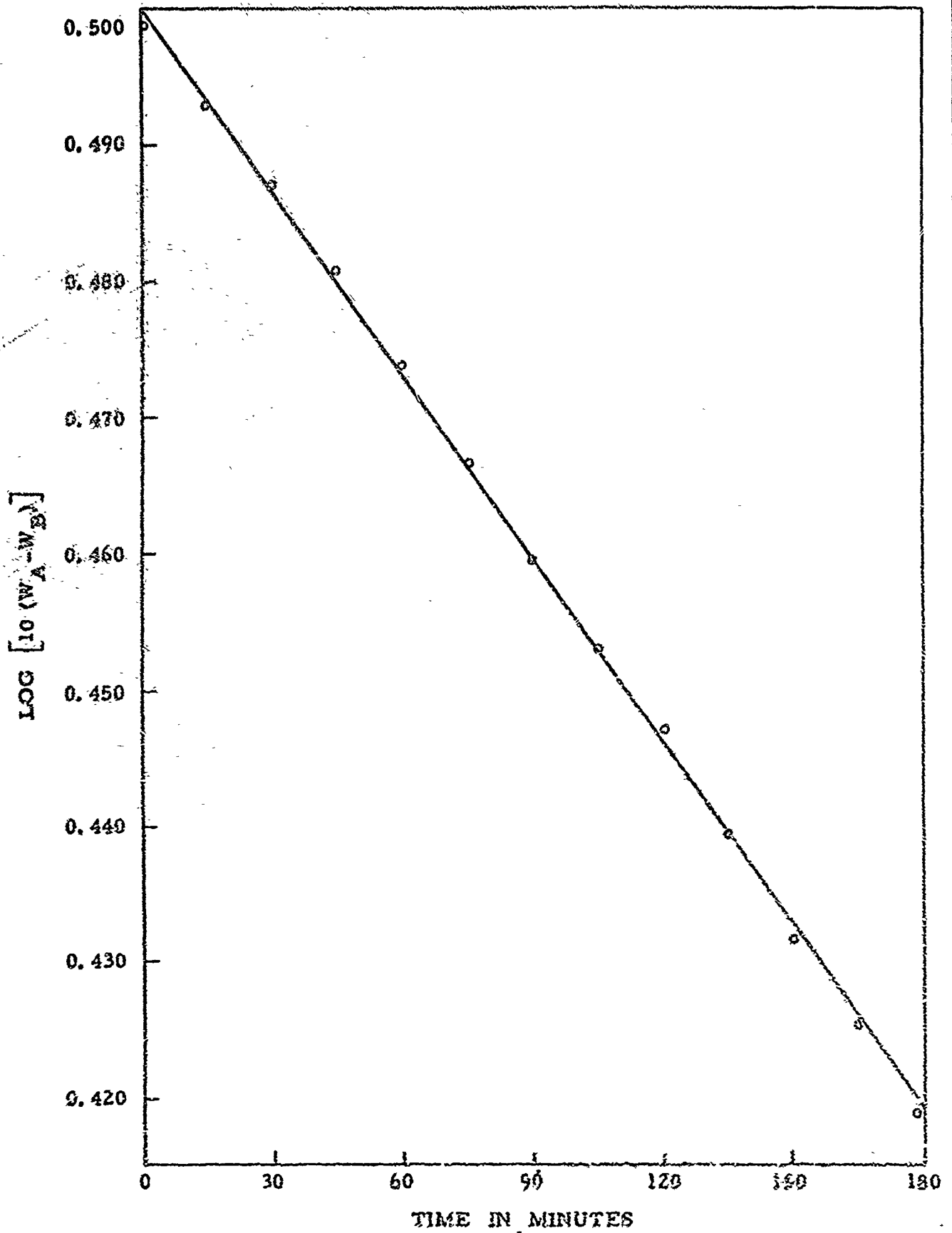


FIGURE 7 - Diffusion Rate-PUDD 600

V. REFERENCES

1. A. R. Gordon, *Ann. N. Y. Acad. Sci.*, 46 285 (1945)
2. E. L. Harris in "Characterization of Separators for Alkaline Silver Oxide Zinc Secondary Batteries", ed. by J. E. Cooper and A. Fleischer, AF Aero Propulsion Laboratory, Wright-Patterson AFB, Ohio, 1964, p. 93
3. T. P. Dirkse, AFAPL TR-64-144, Dec. 1964, p. 5
4. G. Akerlof and P. Bender, *J. Am. Chem. Soc.* 63 1085 (1941)

Security Classification

DOCUMENT CONTROL DATA - R&D

(Security classification of title, body of abstract and indexing annotation must be entered when the overall report is classified)

1. ORIGINATING ACTIVITY (Corporate author) Delco-Remy Division General Motors Corporation Anderson, Indiana		2a. REPORT SECURITY CLASSIFICATION Unclassified	
2b. GROUP			
3. REPORT TITLE Silver-Zinc Electrodes and Separator Research			
4. DESCRIPTIVE NOTES (Type of report and inclusive dates) 1 October 1966 to 1 January 1967			
5. AUTHOR(S) (Last name, first name, initials)			
6. REPORT DATE 15 January 1967		7a. TOTAL NO. OF PAGES	7b. NO. OF REFS
8a. CONTRACT OR GRANT NO. AF33(615)-3487		9a. ORIGINATOR'S REPORT NUMBER(S)	
8b. PROJECT NO.		9b. OTHER REPORT NO(S) (Any other numbers that may be assigned this report)	
10. AVAILABILITY/LIMITATION NOTICES Foreign announcement and dissemination of this report by DDC is not authorized.			
11. SUPPLEMENTARY NOTES		12. SPONSORING MILITARY ACTIVITY Aero Propulsion Laboratory, Research and Technology Div., Air Force Systems Command Wright-Patterson AFB, Ohio	
13. ABSTRACT <p>The use of $ZnSO_4$ in the negative plate mix appears to aid cycle life at 60% depth-of-discharge.</p> <p>Surfactants tested to date other than Emulphogene EC-610 do not improve cycle life performance at room temperature at 60% depth-of-discharge.</p> <p>Development of failure analysis techniques are progressing through the use of one media, the photomicrograph.</p> <p>A first approach to the estimation of degree of molecular hydration in KOH solutions of battery strength is made, and on this basis, limiting values of hydrated ion sizes are calculated.</p>			

DD FORM 1473
1 JAN 64

Security Classification

Security Classification

14	KEY WORDS	LINK A		LINK B		LINK C	
		ROLE	WT	ROLE	WT	ROLE	WT

INSTRUCTIONS

1. **ORIGINATING ACTIVITY:** Enter the name and address of the contractor, subcontractor, grantee, Department of Defense activity, or other organization corporate author, issuing the report.

2a. **REPORT SECURITY CLASSIFICATION:** Enter the overall security classification of the report. Indicate whether "Restricted Data" is included. Marking is to be in accordance with appropriate security regulations.

2b. **GROUP:** Automatic downgrading is specified in DoD Directive 5200.10 and Armed Forces Industrial Manual. Enter the group number. Also, when applicable, show that optional markings have been used for Group 3 and Group 4 as authorized.

3. **REPORT TITLE:** Enter the complete report title in all capital letters. Titles in all cases should be unclassified. If a meaningful title cannot be selected without classification, show title classification in all capitals in parenthesis immediately following the title.

4. **DESCRIPTIVE NOTES:** If appropriate, enter the type of report, e.g., interim, progress, summary, annual, or final. Give the inclusive dates when a specific reporting period is covered.

5. **AUTHOR(S):** Enter the name(s) of author(s) as shown on or in the report. Enter last name, first name, middle initial. If military, show rank and branch of service. The name of the principal author is an absolute minimum requirement.

6. **REPORT DATE:** Enter the date of the report as day, month, year; or month, year. If more than one date appears on the report, use date of publication.

7a. **TOTAL NUMBER OF PAGES:** The total page count should follow normal pagination procedures, i.e., enter the number of pages containing information.

7b. **NUMBER OF REFERENCES:** Enter the total number of references cited in the report.

8a. **CONTRACT OR GRANT NUMBER:** If appropriate, enter the applicable number of the contract or grant under which the report was written.

8b, 8c, & 8d. **PROJECT NUMBER:** Enter the appropriate military department identification, such as project number, subproject number, system numbers, task number, etc.

9a. **ORIGINATOR'S REPORT NUMBER(S):** Enter the official report number by which the document will be identified and controlled by the originating activity. This number must be unique to this report.

9b. **OTHER REPORT NUMBER(S):** If the report has been assigned any other report numbers (either by the originator or by the sponsor), also enter this number(s).

10. **AVAILABILITY/LIMITATION NOTICES:** Enter any limitations on further dissemination of the report, other than those

imposed by security classification, using standard statements such as:

- (1) "Qualified requesters may obtain copies of this report from DDC."
- (2) "Foreign announcement and dissemination of this report by DDC is not authorized."
- (3) "U. S. Government agencies may obtain copies of this report directly from DDC. Other qualified DDC users shall request through _____."
- (4) "U. S. military agencies may obtain copies of this report directly from DDC. Other qualified users shall request through _____."
- (5) "All distribution of this report is controlled. Qualified DDC users shall request through _____."

If the report has been furnished to the Office of Technical Services, Department of Commerce, for sale to the public, indicate this fact and enter the price, if known.

11. **SUPPLEMENTARY NOTES:** Use for additional explanatory notes.

12. **SPONSORING MILITARY ACTIVITY:** Enter the name of the departmental project office or laboratory sponsoring (paying for) the research and development. Include address.

13. **ABSTRACT:** Enter an abstract giving a brief and factual summary of the document indicative of the report, even though it may also appear elsewhere in the body of the technical report. If additional space is required, a continuation sheet shall be attached.

It is highly desirable that an abstract of classified reports be unclassified. Each paragraph of the abstract shall end with an indication of the military security classification of the information in the paragraph, represented as (TS), (S), (C), or (U).

There is no limitation on the length of the abstract. However, the suggested length is from 150 to 225 words.

14. **KEY WORDS:** Key words are technical, meaningful terms or short phrases that characterize a report and may be used as index entries for cataloging the report. Key words must be selected so that no security classification is required. Key words, such as equipment model designation, trade name, project code name, geographic location, may be used as key words but will be followed by an indication of technical context. The assignment of links, prices, and availability is optional.